Provided for non-commercial research and educational use.
Not for reproduction, distribution or commercial use.

This article was originally published in the *Comprehensive Structural Integrity, 2nd Edition* published by Elsevier, and the attached copy is provided by Elsevier for the author's benefit and for the benefit of the author's institution, for non-commercial research and educational use, including without limitation, use in instruction at your institution, sending it to specific colleagues who you know, and providing a copy to your institution's administrator.

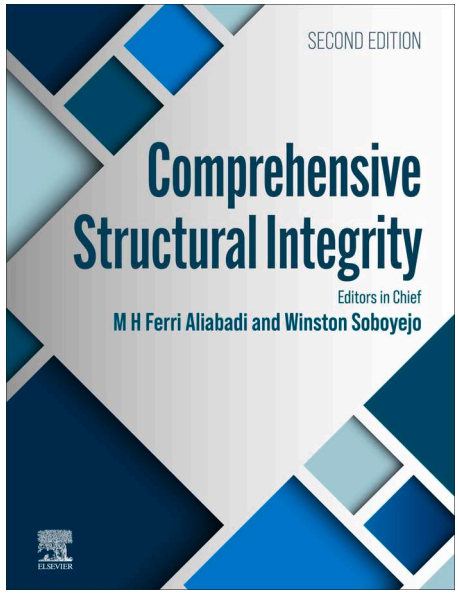

All other uses, reproduction and distribution, including without limitation, commercial reprints, selling or licensing copies or access, or posting on open internet sites, your personal or institution's website or repository, are prohibited. For exceptions, permission may be sought for such use through Elsevier's permissions site at:

https://www.elsevier.com/about/policies/copyright/permissions

Oyewole, Oluwaseun K., Oyelade, Omolara V., Ichwani, Reisya, Koech, Richard, Oyewole, Deborah O., Cromwell, Jaya, Olanrewaju, Yusuf and Soboyejo, Winston O. (2023) Mechanical Properties of Solar Cell Structures. In: Aliabadi, Ferri M H and Soboyejo, Winston (eds.) *Comprehensive Structural Integrity, 2nd Edition,* vol. 10, pp. 185–208. Oxford: Elsevier.

http://dx.doi.org/10.1016/B978-0-12-822944-6.00052-9

© 2023 Elsevier Ltd All rights reserved.

Author's personal copy

Mechanical Properties of Solar Cell Structures

Oluwaseun K Oyewole, Department of Mechanical and Materials Engineering, Worcester Polytechnic Institute, Worcester, MA, United States
Omolara V Oyelade, Department Theoretical and Applied Physics, African University of Science and Technology, Abuja, Nigeria
Reisya Ichwani, Department of Mechanical and Materials Engineering, Worcester Polytechnic Institute, Worcester, MA, United States
Richard Koech, Department Materials Science and Engineering, African University of Science and Technology, Abuja, Nigeria
Deborah O Oyewole, Department of Mechanical and Materials Engineering, Worcester Polytechnic Institute, Worcester, MA, United States
Jaya Cromwell, Department of Mechanical and Materials Engineering, Worcester Polytechnic Institute, Worcester, MA, United States
Yusuf Olanrewaju, Department Materials Science and Engineering, African University of Science and Technology, Abuja, Nigeria
Winston O Soboyejo, Department of Mechanical and Materials Engineering, Worcester Polytechnic Institute, Worcester, MA, United States

© 2023 Elsevier Ltd All rights reserved.

Abstracts

The interplay between mechanical and optoelectronic properties is becoming very interesting reliability evaluation of solar cells. Emerging flexible and stretchable solar cells also required an in-depth understanding of mechanical properties of layered thin film constituents. This article explores the mechanical properties of solar cell structures. The roles of mechanical properties in solar cell structures are presented before elucidating the effects of processing on mechanical properties. The mechanical testing techniques are presented before highlighting the interfacial fracture and its applications in lamination of layered solar cell structures. The salient conclusions are summarized for use in the design of rigid and flexible/stretchable solar cells.

Nomenclature

CTLs Charge transport layers
FPSCs Flexible perovskite solar cells
ITO Indium Tin Oxide
OSCs Organic solar cells
P3HT:PCBM Poly(3-hexylthiophene)
PDMS Poly(dimethylsiloxane)
PEDOT:PSS Poly(3,4 ethylenedioxythiophene):poly(styrenesulfonate)
PEN Polyethylene naphthalate
PET Polyethylene terephthalate

Author's personal copy

PSCs Perovskite solar cells
TCO Transparent conducting oxide

Key Points

- Mechanical reliability of solar cell structures relies on the understanding of mechanical properties.
- The effect of processing conditions on mechanical robustness and reliability of solar cell structures are explored.
- Mechanical characterization techniques for solar cell structures are highlighted.
- The interfacial fracture is the related to lamination of solar cell structures.

Introduction

There has been increase in the demand for energy due to ever-increasing population and industrial exploits. Several sources of energy have been sought for to meet up with this increasing demand. Among many sources are fossil fuels, coal and sun. Fossil fuels have been the common source of energy which is non-renewable in nature and has potential for climate change and global warming as a result of emission of air pollutants from burning fuels. There is, therefore, a need for zero emission green energy to reduce global warming and many other problems associated with it.

A way of solving the global warming problems that are caused by burning of fossil fuels is to replace them with clean renewable energy such as solar energy, wind and hydrothermal energy. Among the renewable sources of energy, sun energy seems to be abundant and can be harnessed and used to drive every sector of the world economy. Renewable energy industry has been dominated by first-generation silicon solar cells that are based on very expensive technologies that make the cost per watt of solar energy to be too high. These silicon solar cells include monocrystalline silicon solar cells which are sliced from large single crystals that are grown under tightly controlled conditions; polycrystalline silicon solar cells that are produced from multiple silicon crystals; amorphous silicon solar cells which are produced in a way that is slightly different from the above, and hybrid silicon solar cells. There is a lot of work going on to reduce the cost of production of silicon based solar cells by using amorphous silicon, Cadmium Telluride (CdTe), (Wu, 2004) and Copper Indium Gallium Telluride (CIGS) (Philip *et al.*, 2010).

Most of the silicon based solar cell are faced with a lot of stress-induced mechanical problems. These include: buckling of front and back contacts; delamination-induced buckling due to thermal mismatch; interfacial fracture problems between contacts and the silicon semiconductor materials; interfacial delamination of encapsulant from cell or modules; interfacial delamination between encapsulant and backsheet, and cracking of the brittle silicon materials. Hence, the understanding of mechanical properties of these materials can help guide the root cause failure in reliability testing of these conventional solar cells in a way that make them last longer.

In an effort to further bring down the cost per watt of solar energy, new solar cell technologies are emerging. These emerging solar cells are referred to as the third-generation solar cells. They are the new class of solar cells which are made from organic and hybrid organic-inorganic materials that are cheap and easy to synthesize. These new solar cells include: organic solar cells, dye-sensitized solar cells, quantum dots solar cells, and perovskites/tandem perovskite solar cells.

In the case of organic solar cells, they are inexpensive and can be made from semiconducting organic materials that can be prepared by simple deposition techniques. Organic materials were found to be promising candidates as they have very strong optical absorption and can be produced using cheap deposition methods (Aziz and Ismail, 2015; Hoppe and Sariciftci, 2004; Krebs *et al.*, 2009; Sun *et al.*, 2018; Zhang *et al.*, 2011) They can be used in applications where light weight, (Kaltenbrunner *et al.*, 2012; Liu *et al.*, 2014) and flexibility (Asare *et al.*, 2015; Kim *et al.*, 2015c; Li *et al.*, 2012; Liu *et al.*, 2014) is important. These materials have been studied over the past three decades (Aziz and Ismail, 2015; Facchetti, 2013; Kaltenbrunner *et al.*, 2012; Krebs, 2009; Li *et al.*, 2012; Meng *et al.*, 2018; Tang, 1986; Yambem *et al.*, 2012) The organic semiconductor materials include conjugated polymers and carbon-based molecules. The conjugated polymers are organic materials that are known to have a backbone chain of alternating double and single carbon-carbon bonds.(Malliaras and Friend, 2005).

Among several photoactive organic semiconductor materials that have been used for organic solar cells (OSCs), bulk heterojunction (BHJ) photoactive structures have shown great potential in OSCs (Akogwu *et al.*, 2011; Jae *et al.*, 2008; Kim *et al.*, 2011; Lipomi *et al.*, 2011; Oyewole *et al.*, 2020; Venkateswararao *et al.*, 2018). They have tunable electron donor and electron acceptor materials that are intimately mixed in a bulk volume to form the photoactive layer. Most of the world record OSCs have had BHJ architectures with improved power conversion efficiencies ranging from 2% to 17% (An *et al.*, 2020; Jae *et al.*, 2008; Lin *et al.*, 2020; Zhao *et al.*, 2017).

It is important to note that the underlying mechanical properties of the layered OSCs is essential for the design of robust structures that can flex or stretch. The mechanical properties are also important for the design of OSC structures that have high interfacial integrity for enhanced charge transportation within the OSCs. Mechanical stability of OSCs depends on the intermolecular interaction and surface forces within the photoactive organic materials which can sometimes control device degradation.

Perovskite Solar Cells (PSCs) are another types of emerging solar cells that have a hetero-junction kind of structures which are formed by stacking different layers of semiconducting materials together in a planar or mesoscopic architecture (Pascoe *et al.*, 2016).

Author's personal copy

These solar cells have revolutionized the field of photovoltaics (PV) due to their excellent photophysical properties and low cost (Zarick *et al.*, 2018). Their photoactive layer takes the ABX_3 structure of perovskites with their excellent photophysical properties (Manser *et al.*, 2016; Sum and Mathews, 2014). The active layer can be processed easily from precursor solutions and have tunable properties that make them suitable for diverse applications (Wang *et al.*, 2019b). They can also be deposited on flexible and stretchable substrates which make the overall PSC devices to accommodate strains during bending or stretching. Perovskite solar cells can, therefore, be produced in a way that meet the high rising need of mechanically compliant, miniature, and light weight solar energy harnessing systems that can easily be integrated into curved surfaces, building facades, wearable and portable electronics, and space crafts.

As PSC devices transit from the laboratory protypes to real large-scale applications, mechanical robustness becomes an important consideration. The fabricated PSC devices should be robust enough with considerable good mechanical properties to tolerate any mechanical deformation they may encounter during handling and while under operation in the ambient environment without experiencing any significant deterioration of their photovoltaic performance. Development of flexible perovskite solar cells (FPSCs) that are stable under mechanical deformations has attracted recent research attentions (Popoola *et al.*, 2018; Roldán-Carmona *et al.*, 2014; Yang *et al.*, 2019). The understanding of mechanical properties, such as tensile modulus, ductility, film and interfacial fracture toughness, and many other mechanical parameters are of great importance in designing reliable FPSCs.

The main approaches that have been exploited to develop FPSCs include the use of flexible substrates and the engineering of the overlying device components such as the electrodes, charge transport layers (CTLs) and the perovskite films (Hu *et al.*, 2021; Liang *et al.*, 2021; Lim *et al.*, 2021; Yang *et al.*, 2019). The use of flexible substrates is the first and foremost step in developing mechanically robust FPSCs (Jung *et al.*, 2019; Li *et al.*, 2016; Liang *et al.*, 2021). The substrate also enables the flexibility of PSCs, while reducing the residual strains in the perovskite film. It also increases the power output per unit weight of the overall PSC device, thus widening the scope of their application (Kaltenbrunner *et al.*, 2015). The substrate, however, has to be optically transparent, impervious to water and oxygen, chemically inert to solvents, able to retain their properties after being subjected to some levels of deformations, and should possess excellent surface, thermal and thermomechanical properties so that the PCE and long-term stability of PSC will not be affected (Asare *et al.*, 2020; Jung *et al.*, 2019). There are different forms of substrates that have been used in the fabrication of FPSCs but the polymeric substrates such as polyethylene terephthalate (PET), polyethylene naphthalate (PEN), polydimethylsiloxane (PDMS), polyethersulfone (PES), and polyimide (PI) foils are commonly used due to their excellent flexural, optical and solvent resistance properties (Zardetto *et al.*, 2011).

The use of polymeric substrates restricts the annealing temperatures for the overlying layers, an issue that is responsible for the low power conversion efficiencies of FPSCs. It is also the reason why FPSCs mostly take a planar and inverted device configuration, eliminating the need for sintering for the mesoporous layer. Indium doped tin oxide (ITO)-coated PET and PEN substrates are mostly used as the base for FPSCs, though the presence of ITO has been shown to limit their good performance under high levels of mechanical deformations. In applications requiring higher flexibility, the commonly used transparent conductive oxide (TCO)-based electrodes and CTLs can act as weakest points for crack initiation, contributing to the failure of FPSCs under mechanical distortions (Kim *et al.*, 2015a).

In an attempt to address this issue of brittleness of the TCO, carbon based materials, silver nanowires and highly conductive poly(3,4 ethylenedioxythiophene):poly(styrenesulfonate) (hc-PEDOT:PSS) have been used as transparent electrodes in place of the brittle ITO (Chen *et al.*, 2017; Tang *et al.*, 2019; Zhang *et al.*, 2018b). Exploiting the inverted planar PSC device structure has also allowed the use of low temperature processable organic hole transport layers (HTLs) that can serve as both transparent conductive electrode and HTL in FPSCs (Dianetti *et al.*, 2015; Galagan *et al.*, 2011; Zhang *et al.*, 2018a). Highly conductive PEDOT:PSS has proved to be the best material for use in flexible electronic structures (including FPSCs) due to its high optical transparency and good electrical conductivity (Fan *et al.*, 2019; Huseynova *et al.*, 2019). To improve the mechanical integrity of hc-PEDOT:PSS, appropriate proportions of polymeric compounds such as polyethylene oxide (PEO) can be added (Lee *et al.*, 2018). For metallic thin film electrodes, the use of liquid metals that can accommodate mechanical distortions such as eutectic indium gallium (Eu-InGa) has received great considerations.

With much stride having been made with the substrates, CTLs and electrodes, the greatest impediment towards achieving a fully flexible or stretchable PSC devices currently lies in the perovskite layer. Through nano- and micro-indentation tests, perovskite films have been shown to exhibit low fracture resistance and low fracture energies even in the absence of grain boundaries (Rakita *et al.*, 2015; Tu *et al.*, 2018). This means that they are highly susceptible to mechanical failures during deformation (Rolston *et al.*, 2016). The mechanical properties of perovskite films are strongly influenced by the strength of B-X bonds, the magnitude of hydrogen bond between the A-site cations and the halides, the packing density and the microstructure (Sun *et al.*, 2015). Therefore, the perovskite stoichiometry, precursor chemistry, the preparation conditions and the interface mechanics are the key parameters in mechanical stability of PSCs (Dong *et al.*, 2021a; Rolston *et al.*, 2016, 2018).

The mechanical stress state of the perovskite films can have some impact on their optoelectronic properties. The mechanical stability of perovskite films can be quantified by determining their Young's moduli and hardness. The bulk modulus decreases as the ionic radius of A cuboctahedron group increases. Dimensionality tailoring has also been shown to be effective in tuning the elastic modulus of perovskite films. 2D perovskites are known to exhibit lower elastic moduli and higher ambient stabilities relative to their 3D counterparts though their PCE is lower (Gao *et al.*, 2020).

By using a combination of experiments and DFT calculations, Rathore *et al.* (2021) have shown that the elastic modulus of perovskite films can be reduced from about 16.5–6.3 GPa, if transformed from 3D to 2D perovskite. They have also shown that the mechanical integrity and environmental stability can be improved by mixing pure 3D and 2D perovskites to obtain moved 2D-3D perovskites (Rathore *et al.*, 2021). It has also been demonstrated experimentally that the intercalation of polymers into the perovskite lattice can effectively modulate its mechanical robustness. Xiong *et al.* (2018) have modified the perovskite film in PSC with polyvinylpyrrolidone (PVP) polymer that led a marked improvement in its mechanical robustness. The PCE of the polymer-modified

Author's personal copy

PSC could remain stable after 600 h in a highly humid environment and the device could also retain over 73% of its PCE after 1000 bending cycles. The polymeric compounds in the perovskite films will form cross-linking network that will absorb any mechanical strain thus improving their tolerance of various mechanical deformation modes.

This article presents the mechanical properties that are essential for the designs of robust solar cell structures. The introduction and the general overview of the solar cells are presented in section "Introduction" before elucidating the mechanical properties that are key to the design of efficient and robust silicon based solar cells, organic solar cells, dye sensitized solar cells, perovskite solar cells and flexible and stretchable solar cells in section "Effects of Mechanical Properties in Silicon and Emerging Solar Cells". The effects of material processing and material selection on mechanical properties of layered solar cells are explored in section "Effects of Processing on Mechanical Properties of Solar Cell Structures". The various mechanical testing techniques for solar cell structures are presented in section "Mechanical Testing Methods and Analysis in Solar Cells" while the typical interfacial mechanical fracture due to stress-induced deformation in layered solar cells is presented in section "Interfacial Fracture in Layered Solar Cell Structures". The salient concluding remarks and summary are then presented in section "Summary and Concluding Remarks".

Effects of Mechanical Properties in Silicon and Emerging Solar Cells

The interplay of mechanical property and performance reliability is very critical for production of affordable solar cells that are reliable and available for a wide range of applications. In the case of conventional silicon solar cells, the understanding of mechanical properties of different assembled components is very crucial for reliability of cells and modules in the field where they are being exposed to several environmental changes. These components include: the brittle silicon materials, front and back contacts, backsheet materials, laminating materials just to mention but a few. There is, therefore, a need to build a mechanically robust solar cells with strong components that can withstand stress-induced failure when exposed to different environmental conditions such as snow, wind and other effects. The knowledge of mechanical behavior is also more pertinent to emerging solar cells such as organic and perovskite solar cells since they can be made flexible and stretchable for many applications.

A more comprehensive understanding that explores the mechanical properties of these solar cells and how they relate to their optoelectronic properties is, therefore, required for robustness, enhanced performance and reliability. In the case of flexible/stretchable solar cells, the mechanical properties, as well as mechanical failure mechanisms, play a key role in module roll-to-roll productions. Furthermore, the active materials must be able to tolerate certain mechanical strains to be fabricated on ultrathin plastic substrates. The range over which mechanical properties vary will have a substantial impact on the solar cells' long-term stability. Some mechanical properties that affect the performances of solar cells include Young's modulus, hardness, ductility and fracture toughness. This section explores these properties as they interplay with the optical and electrical behavior of solar cells.

Conventional Silicon Solar Cells

For a variety of reasons, single or large-grained multi-crystalline silicon is the most common photovoltaic material. To increase throughput and production yield for crystalline silicon solar cells to meet future energy demands, there is a major need for system cost reductions and manufacturing advancements. Using thinner silicon wafer is one way to cut costs. However, silicon solar cells suffer from a high rate of breaking because of the thickness reduction. Residual stresses are also inevitable in silicon solar cells due to mismatch in thermal expansion coefficients of the materials employed in the metallic connections. It is important to note that when the wafer cools, it bends and creates a convex or concave body which fracture when mechanically loaded. It's critical to find a balance between the performance characteristics, strength, reliability and price.

The mechanical properties of silicon solar cells have been found to be dependent on the crystallinity and grain size. When subjected to four-point bending tests, the mechanical strengths of the silicon wafers with large grains are higher than those with smaller grain size.(Dragišić, 2015) **Table 1** presents the effects of crystallinity on the strength of silicon wafers. The low strength in the wafers with smaller grains can be associated with the nucleation and growth of cracks from the several grain boundaries during deformation. Hence, the performance characteristics of silicon solar cells are affected by the grain size and crystallinity type of silicon with low strength, making it difficult for such silicon-based solar cells to withstand variational loads due to wind and other environmental loadings such as snow.

Table 1 Mechanical strengths of silicon wafers of different type of crystallinity

Type Crystallinity	*Strength (MPa)*
Twin boundary	274
Triple junction	268
Many grains	251

Note: Reproduced from Dragišić, V.T., 2015. Silicon solar wafers: Quality control and improving the mechanical properties. Procedia Engineering 117 (1), 459–464.

Author's personal copy

Table 2 Elastic modulus of photoactive P3HT:PCBM

Ratio	*Tensile modulus*
1:0.8	6.02 ± 0.03
1:1	4.3
1:0.5	2.02 ± 0.48

Note: Reproduced from Suchol Savagatrup, A.D.P., O'Connor, T.F., Zaretski, A.V., *et al.*, 2014. Mechanical degradation and stability of organic solar cells: Molecular and microstructural determinants. Energy & Environmental Science 8 (1), 55–80.

Organic Solar Cells

Organic solar cells are a promising low-cost, lightweight, and flexible alternative to conventional solar cell technology. Power conversion efficiencies of over 10%, (Dou *et al.*, 2013) estimated lifetimes of over seven years for devices on rigid substrates, power-to-mass ratios of 10 W g^{-1}, and projected energy payback durations on the order of days are among the benefits realized by OSCs (Espinosa *et al.*, 2012). Due to a greater understanding of device physics, superior materials, and wiser layouts, the relatively low efficiencies of different organic solar cell technologies are continuously improving. The creation of flexible and physically resilient necessitates a thorough understanding of the heterogeneous material stack's mechanical behavior.

Prior work on mechanical properties of organic semiconductors shows that device responses to mechanical deformation are considerably varied (Lipomi and Bao, 2011; Suchol Savagatrup *et al.*, 2014). The intermolecular and surface forces present in the organic semiconductors and auxiliary layers, and how they influence the characteristics of thin films, are the factors that influence the mechanical stability of OSCs. Tensile tests and nanoindentation have been used to measure the mechanical properties (ultimate strength and tensile modulus) of conjugated polymers (Koidis *et al.*, 2013a,b). Due to unsaturated intermolecular interactions at interfaces and confinement of a plastic zone at the crack tip after decohesion of layers sandwiched between relatively stiff substrates, organic films can have thickness-dependent mechanical characteristics (Dennler *et al.*, 2007).

The mechanical properties of organic thin films are consequently not always representative of the properties of macroscopic samples in all dimensions. (O'Connor *et al.*, 2010) Organic films with thicknesses $\leq 100nm$ tend to confound measurements by direct tensile testing because of the difficulty in producing and manipulating free standing film and defect concentrated stress that dominate the mechanical response. Nanoindentation has yielded qualitative and relative data that has been valuable, but the precision of the measured properties is restricted by the convolution of the effect of the substrate, viscoelastic behavior of the polymer, the uncertainty of the tip size and contact area of the scanning probes. Mechanical buckling is effective in measuring the tensile modulus of a variety of organic films. (Koidis *et al.*, 2013a,b).

In the case of P3HT:PCBM-based organic solar cells, the mixing ratio has been shown to have a significant effect on mechanical property which also interplay with the processing temperature (Suchol Savagatrup *et al.*, 2014). For typical mixing ratios of P3HT:PCBM (**Table 2**), the tensile modulus is low when less proportion of the brittle PCBM is incorporated into the blend. The performance of organic solar cells has also been shown to be dependent on the elastic modulus.(Awartani *et al.*, 2013) It shows that the efficiency of organic solar cells increases with increasing modulus (**Fig. 1**(a)) (Awartani *et al.*, 2013). It is important to note that active blends with higher proportion of PCBM has higher modulus. This increase can be associated with improvement in the crystallinity and microstructures of the blended materials which enhance charge transportation. However, due to brittle nature of the PCBM, the blend with high elastic modulus (with higher efficiency) has been shown to exhibit low crack onset strain (Awartani *et al.*, 2013). It is, therefore, very important to balance the mechanical properties of organic solar cells in flexible/stretchable applications.

Perovskite Solar Cells

Hybrid organic-inorganic perovskites (HOIPs) is a type of material that is continuing to change the area of photovoltaics, with devices now achieving power conversion efficiencies of above 25.2% (NREL, 2020). HOIPs are a type of material that has a composition ABX_3, where the $A = CH_3NH_3^+$ (MA^+), $CH(NH_2)_2^+$ (FA^+), or Cs^+, $B = Pb^{2+}$ or Sn^{2+}, and $X = I^-$, Br^-, or Cl^-. Long lifetimes, good charge carrier mobilities, tunable bandgaps, and high extinction coefficients are the remarkable characteristics of HOIPs solar cells (Wu *et al.*, 2018). The ease with which HOIPs are processed from solution opens the possibility of their use in thin-film devices other than photovoltaics, such as flexible and wearable electronics and other strain-intensive applications (Docampo *et al.*, 2013).

The HOIPs have also demonstrated exceptional performance in light-emitting diodes, ultra-lasers, and photodetectors (Murali *et al.*, 2016). The desire to fabricate flexible solar cells and design pressure-assisted solar cells motivate the need to study the mechanical properties of layers in model perovskite solar cells. Hence, the mechanical stability and deformation behavior HOIPs are receiving more attention. Computational investigation of $MAPbI_3$ fracture indicated that it is more compressible and ductile than inorganic perovskites, suggesting the possibility of its usage in wearable devices (Yu *et al.*, 2016). Density functional theory (DFT) calculations on HIOPs' mechanical property measurements revealed Young's moduli in the range 10–20 GPa (Feng, 2014). Prior research (Ma *et al.*, 2021; Rakita *et al.*, 2015; Reyes-Martinez *et al.*, 2017; Sun *et al.*, 2015) has employed nanoindentation to characterize the characteristics of HOIPs to get Young's moduli and hardness values, which support theoretically estimated values.

Author's personal copy

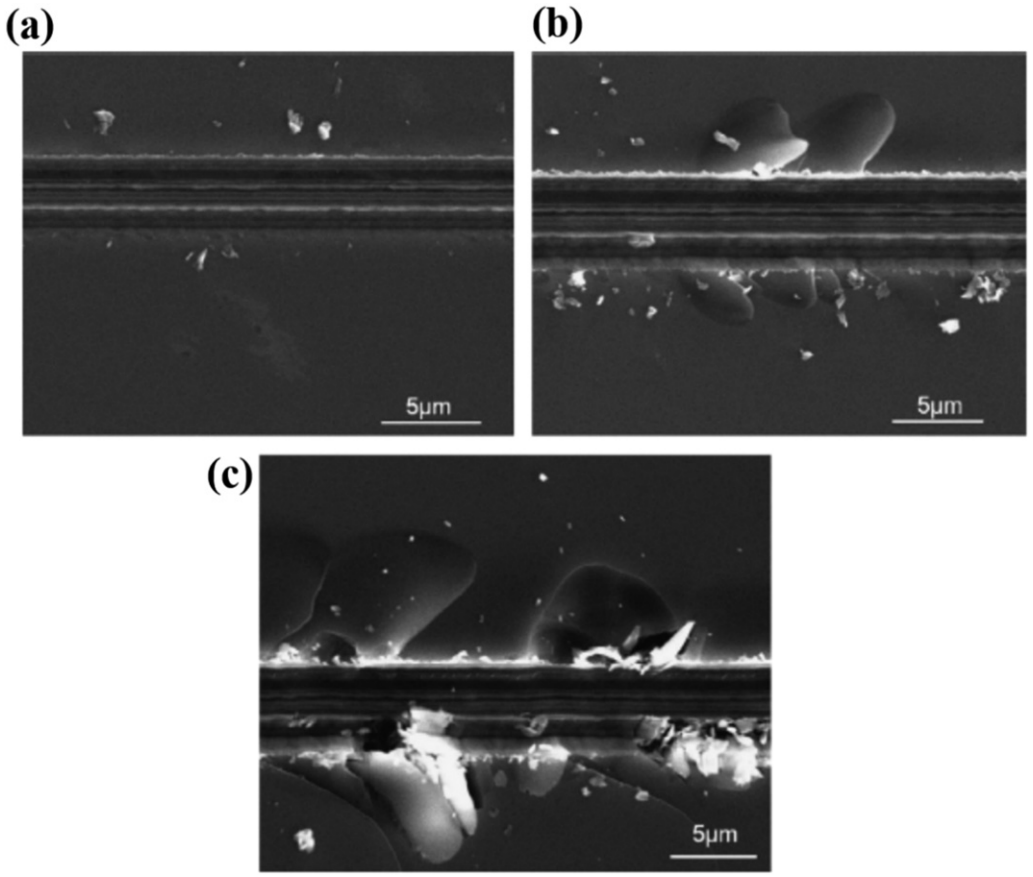

Fig. 1 Surface morphology produced in diamond scribing at depths of (a) 0.15 mm, (b) 0.27 mm, and (c) 0.40 mm, showing greater brittle fracture at larger depths Reprinted from Wu, H., Melkote, S.N., 2013. Effect of crystal defects on mechanical properties relevant to cutting of multicrystalline solar silicon. Materials Science in Semiconductor Processing 16 (6), 1416–1421.

These findings contribute to a better understanding of HOIPs solar cells that can endure mechanical deformations and its usage in pressure-assisted fabrication (Oyelade *et al.*, 2020).

Effects of Processing on Mechanical Properties of Solar Cell Structures

The mechanical properties of solar cell structures can influence their performance, robustness for storage, transportation and installation and ultimately their useful lifetime. Understanding these properties and how they are influenced, improved or even worsened by device processing is important to the manufacture and increase ng deployment of solar cells in the use of solar energy. This section presents the effects of processing on the mechanical properties of different types of solar cells.

Processing of Silicon Solar Cells

Silicon solar cells are commonly produced as wafers. Cracking or breakage of these wafers (Popovich *et al.*, 2013) in various stages from production to usage can cause device failure. Thinner devices can be more desirable (Gouttebroze *et al.*, 2013) as they are cheaper, but they are more prone to breakage (Popovich *et al.*, 2011). Processing and crystallinity affect the fracture strength of silicon solar cells (Popovich *et al.*, 2011). Assembled silicon solar cells can have varying fracture strengths depending on the direction of their loading (Kaule *et al.*, 2014).

The mechanical properties of silicon wafers fabricated by different means varies (Gouttebroze *et al.*, 2013). The materials that were compared were sintered powdered silicon, multi-crystalline silicon from casting, monocrystalline silicon produced by Czochralski process and silicon wafers produced by thermal spraying (Gouttebroze *et al.*, 2013). A ring-on-ring structure was used to determine the bending strength of the different wafers. The measurements showed that the thermally sprayed silicon wafers had the highest fracture strength followed by the single crystalline wafer, then the multi-crystalline wafer and finally the sintered silicon had the lowest fracture strength.

Silicon wafers can be cut from ingots and this cutting can introduce cracks that can initiate failure (Popovich *et al.*, 2013). The factors that influence fracture strength of the silicon wafers include saw damage, surface roughness, cracks at the edges and grain

Author's personal copy

boundaries (Popovich *et al.*, 2013). This fracture strength has been investigated experimentally (Popovich *et al.*, 2013) by four-point bending. The cutting of the silicon wafers with a saw caused phase transformation that resulted in areas with amorphous silicon and others with polycrystalline silicon. It also results in internal residual stresses where bits of material have been removed. Saw damage resulted in lower fracture strength. Surface roughness due to cutting or etching also reduced fracture strength. Crystallinity also influenced mechanical properties, as more grain boundaries resulted in reduced fracture strength.

Whereas multi-crystalline silicon has a lower fracture strength than single crystalline silicon, a greater dislocation density within grains correlates with a higher fracture toughness when during sawing (Wu and Melkote, 2013). At room temperature silicon is brittle but if it is sawed slowly enough it can behave in a ductile manner. Ductile cutting results in a smooth surface with no cracks as opposed to brittle fracture which yields surface cracks. With increasing depth of the cut there is increasing brittle fracture as shown in **Fig. 1**(a)-(c). At a depth of 0.15 mm there is little evidence or cracks forming alongside the cut. At a depth of 0.27 mm, there are more cracks and silicon fragments alongside the cut. Whereas at 0.4 mm there is significant crack formation and silicon fragmentation beside the cut. However greater dislocation density increases the depth of the cut before the onset of brittle fracture. This has implications for improved cutting of wafers during processing.

Processing of Organic Solar Cells

Organic solar cells are based on polymer materials (Li *et al.*, 2011) which can be deposited as thin films. The fabrication processes include solvent deposition techniques like roll-to-roll printing (Koidis *et al.*, 2013a,b), spin coating (Wang *et al.*, 2013), and blade coating (Ye *et al.*, 2018). Their properties can be studied by nanoindentation which can be used to investigate a range of thin film materials (Gerthoffer *et al.*, 2017). It is very important to have a good understanding of mechanical properties of organic solar cells for robust stretchable organic solar cell structures that can be deposited on stretchable substrate like poly(dimethyl-siloxane) (PDMS) (Oyewole *et al.*, 2020).

Varying the processing conditions and protocol of organic solar cells can affect their mechanical properties. (Karagiannidis *et al.*, 2011; Li *et al.*, 2011) In the case of poly(3-hexylthiophene) (P3HT) and [6,6]-phenyl C61-butyric acid methylester (P3HT:PCBM), the proportion of the blend components as well as the processing conditions can affect its mechanical property. These processing conditions include: film drying rate, the annealing temperature and the annealing time (Li *et al.*, 2011). Li *et al.* have estimated the Young's modulus and the hardness of P3HT:PCBM, while the best Power Conversion Efficiency (PCE) was also measured for a 1:1 ratio of P3HT to PCBM at an annealing temperature of 110°C for 10 min. These corresponded to the lowest Young's modulus 20.73 GPa and the lowest hardness 649 MPa of all the processing parameters.

Introduction of additives into the active layer of organic solar cells has been shown not to only improve the electrical performance but also alter their mechanical properties (Wang *et al.*, 2013). The introduction of carbon nanotubes (SWCNT) to the active layer of P3HT:PCBM solar cells was used to tune the surface roughness, hardness and Young's modulus. The hardness and Young's modulus increases with increase in the percentage of SWCNT in the P3HT:PCBM. The surface roughness was obtained by Atomic Force Microscopy (AFM) measurements. Moreover, by comparing all-polymer solar cells with PCBM-based polymer solar cells under a double cantilever beam deformation (**Fig. 2**(a)-(b)), (Kim *et al.*, 2018) the fracture resistance of all-polymer solar cells is higher than PCBM-based solar cells. This can be associated with the ductile behavior of the all polymer structures which can accommodate large plastic deformation before the growth of crack. In the case of PCBM-based polymer solar cells, brittle nature of aggregated PCBM can constitute weak interaction between the PCBM and polymer which can lead to low resistance to failure.

Processing of Perovskite Solar Cells

Single crystal perovskite

Different materials and processing conditions have been used for fabrication of perovskite solar cells. It is, therefore, very important to understand how the mechanical properties of these different materials that processed at different conditions interplay. The mechanical

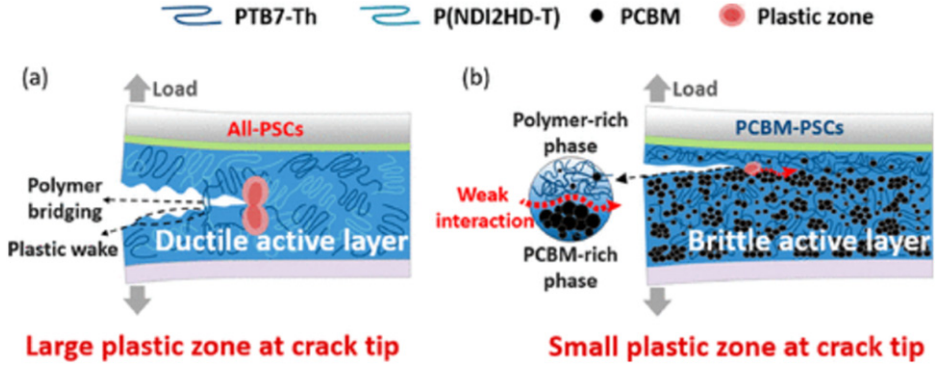

Fig. 2 Schematics of decohesion mechanism of (a) all-Polymer solar cells and (b) PCBM–based polymer solar cells Reprinted from Kim, W., Choi, J., Kim, J.-H., *et al.*, 2018. Comparative study of the mechanical properties of all-polymer and fullerene–polymer solar cells: The importance of polymer acceptors for high fracture resistance. Chemistry of Materials 30 (6), 2102–2111. With permission from American Chemical Society.

Author's personal copy

properties of single crystal perovskites have been studied by nanoindentation (Reyes-Martinez *et al.*, 2017; Sun *et al.*, 2015) to determine properties like Young's modulus and hardness as well as measuring creep and stress relaxation. The introduction of different halides into the perovskite crystal lattice changes the mechanical properties and texture. By studying the single crystalline methyl ammonium lead halide ($CH_3NH_3PbX_3$ where X = I, Br and Cl), (Sun *et al.*, 2015) suitable facets on the crystals have been identified using nanoindentation technique, with the {100} and {110} planes being used with bromine and chlorine as the halide atom and the {100} and {112} planes when iodine was the halide atom. The Young's moduli of $CH_3NH_3PbI_3$ were 10.4 GPa and 10.7 GPa for the {100} and {112} planes respectively. The Young's moduli of $CH_3NH_3PbBr_3$ were 17.7 GPa and 15.6 GPa for the {100} and {110} planes respectively. The Young's modulus of perovskite crystal with bromine modulus and hardness compared to the crystals with iodine as the key.

Perovskite films

Perovskite films can be deposited onto rigid and flexible substrates by spin coating (Dualeh *et al.*, 2014; Gao *et al.*, 2019). Environmental conditions like moisture (water vapor) can lead to the degradation of perovskite films and solar cells (Mamun *et al.*, 2018). The degradation of perovskite films due to exposure to air with 40% humidity for up to 60 h has also been studied (Mamun *et al.*, 2018). The evolution of the elastic modulus and the hardness was examined by nanoindentation. SEM images were taken of the film size to determine changes in grain size. It was found that elastic modulus and hardness increased over the first 27 h then declined up to the 60 h measured. SEM images and XRD data showed that these changes correlated with an increase in grain size and crystallinity in the first 27 h. Subsequently there was chemical degradation and the formation of pinholes.

In 2D perovskites, a single layer of perovskite molecules is separated by a layer or layers of organic molecules (Tu *et al.*, 2018). Two different layered solar cell architectures have been studied using 2D/3D Formamidinium – Lead – Iodide (Thote *et al.*, 2019) as an active layer. They found that the inverted configuration had a better performance, because of lower crack formation due to the underlying layer being better at relieving transverse stresses in the perovskite layer.

Mechanical Testing Methods and Analysis in Solar Cells

Solar cells experience deformations such as bending, stretching and twisting when they are under service condition. To understanding the mechanical behavior and the stress-induced reliability of solar cells, mechanical testing is very crucial for estimation of stress, strain, interfacial adhesion, strength, fracture resistant and toughness. These mechanical properties are so key to the development of deformable solar cells that can bend and stretch (White *et al.*, 2013). The investigation of the physical properties and electrical structures of solar cells, particularly in the emerging organic and hybrid organic–inorganic perovskite (HOIP) solar cells, stimulates efforts to relate material properties to performance (Lipomi, 2016; Liu *et al.*, 2013; Sun *et al.*, 2013). These solar cell structures are made up of different thin films and interfaces that have considerably lower fracture resistance than typical engineering materials used in bulk. Hence, solar cells performance under mechanical stability and deformation behavior is receiving more attention.

In the case of organic and HOIP solar cell structures, applied mechanical stress under the manufacturing and operating conditions can cause crack initiation that can lead to catastrophic fracture (Krebs *et al.*, 2010). The initiation and growth of the cracks initiated under mechanical load can severely affect the efficiency and reliability of cells or modules. Therefore, to understand and enhance the mechanical properties of electronic materials, each layer should be studied for its contribution to solar cell strength. Some of the mechanical properties that are relevant to electronic structure include elastic modulus (typically determined as the tensile or Young's modulus), yield point, toughness, interfacial fracture and strain to fracture (Awartani *et al.*, 2013; O'Connor *et al.*, 2010; Printz *et al.*, 2015; Tank *et al.*, 2009). These properties are governed not only by the structure of individual molecules, but also by how these molecules are arranged in solid form. (Awartani *et al.*, 2013; O'Connor *et al.*, 2010).

Since the whole thickness of HOIP solar cell structure is about 1 μm and therefore difficult to handle the materials, evaluation of the mechanical properties of the layered thin films presents unique problems (JY *et al.*, 2011; Stafford *et al.*, 2004). Tensile mechanical testing specimens for organic and HOIP solar cell structures are usually prepared by fabricating the layered thin films on polymeric substrate (Sun *et al.*, 2015). Another way of measuring the mechanical properties of these electronic structures precisely and more accurately is the development of innovative nano-indentation testing methods (Cheacharoen *et al.*, 2018; Dimesso *et al.*, 2014; Feng 2014; JY *et al.*, 2011; Stafford *et al.*, 2004; Sun *et al.*, 2015).

In the case of brittle silicon based solar cells, four-point bending test is usually deployed to check for stress-induced failure in a way that mimic the environmental effects that the cells or modules experience in the field during snowy or windy weather. The robustness of interfacial interaction between encapsulant and devices is also very key to reliability of solar cell devices. Peel test technique is usually used to test for interfacial adhesion force between the cells and the encapsulant. There is also a unique Brazil testing technique for interfacial fracture in layered thin film structure of solar cells. Most importantly, fatigue behavior of solar cells under stress-induced deformation is essential for lifetime prediction of the devices. The stress-induced deformation can be as a result of thermal exposure or physical bending or stretching. Some of these most common mechanical testing methods for solar cells will be discussed in this section.

Tensile Test and Analysis

Tensile test refers to a situation in which the force (load) is applied in a uni-direction throughout the gauge section. It offers essential mechanical properties such as elastic modulus (stiffness), strain at fracture (ductility), tensile strength, and toughness,

Author's personal copy

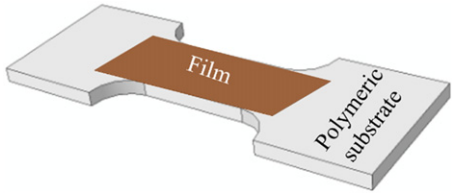

Fig. 3 A typical sample specimen for thin film mechanical testing.

which are necessary for solar cell mechanical design and lifespan. Consequently, with the advent of flexible/stretchable electronics for solar cells that are mechanically deformed in operation, mechanical property assessment is becoming increasingly essential (Krebs *et al.*, 2010). The tensile modulus is calculated from the mechanical response of the stress-strain curve acquired by tensile testing in the initial elastic regime. These properties may be measured by using different methodologies, which depend on the amount of material available and the forms in which it can be processed. In order to evaluate the mechanical properties of organic-inorganic electronics for flexible applications, the component layers are exposed to tensile strain by bending or stretching.

Measurement of the uniaxial tensile properties of free-standing perovskite materials is one of the best ways to overcome the limitations of nanoindentation and DFT studies, since the gauge section will include all possible defects present in film-type perovskite materials. This includes their effects on the resulting tensile properties, thus reflecting the real mechanical properties of the perovskite materials. Another benefit is that solid mechanics can anticipate the deformation behavior of perovskite materials in any distorted state of the solar cell using their tensile properties as input. Models informed by data acquired in both uniaxial tension and compression, in particular, are significantly more likely to anticipate the stresses associated with complicated loading situations. Data from different stress and strain states is more valuable in determining cause and effect connections between the microstructure and mechanical characteristics (Yu *et al.*, 2016). As a result, several tensile testing methods have been employed in order to examine the mechanical properties of organic-inorganic semiconducting thin films.

For thin films of layered organic and HOIP solar cell structures, tensile tests are carried out by depositing the film on an elastomeric substrate since the thickness of each of the layers is in nanoscale. The polymeric substrate is usually a low modulus material that more deformable and can minimize interfacial stresses. A typical sample of the tensile specimen for thin film is shown in **Fig. 3**. However, if more material is available for a conventional pull test, a typical specimen may be cast into the proper size and shape (e.g., dog-bone), and its force-displacement curve can be recorded and translated into its stress-strain curve using the sample's dimensions (Müller *et al.*, 2007).

In the case of tensile test for organic and HOIP cell structure, Kim *et al.* (2015a,b,c) have pioneered the use of a water-based pull test, in which a film is deposited on a flat substrate and then gently floated onto the surface of water. A force vs displacement plot is obtained using a very sensitive load cell connected to a linear actuator. To ensure that the contacts do not tear the delicate thin film, slabs of poly-(dimethylsiloxane) (PDMS) that adhere to the top surfaces of the termini of the floating thin films via van der Waals forces are employed in place of a clamp, minimizing mechanical damage. The water-based method has been used to quantify the stress-strain behavior of P3HT as a function of regioregularity (Root *et al.*, 2017) (the films become more deformable as regiorandomness increases, though charge-carrier mobility decreases) and of all-polymer active layers for intrinsically stretchable solar cells. Because the water-based technique does not bind the film to a solid substrate, the findings may be affected by concentrations of strain in thin regions and flaws within the thin film (Rodriquez *et al.*, 2017).

The monotonic deformation of perovskite materials for solar cells have also been studied. Ahn *et al.* (2019) have reported the uniaxial tensile properties of four perovskite materials; $MAPbI_3$, $MAPb(I_{0.87}\ Br_{0.13})_3$, and two solvent annealed versions of $MAPb(I_{0.87}\ Br_{0.13})_3$. The in-situ testing configuration, stress-strain curves and the images of the fracture surfaces are presented in **Fig. 4**(a)-(d). According to their findings, the tensile fracture strength of $MAPbI_3$ is 33% larger than that of $MAPb(I_{0.87}\ Br_{0.13})_3$ by 33% while the elastic deformation limit for $MAPbI_3$ was 1.17 ($\pm$ 0.13)% and 1.05 ($\pm$ 0.10)% for heat treated $MAPb(I_{0.87}\ Br_{0.13})_3$, which was found to be independent of grain size for $MAPb(I_{0.87}Br_{0.13})_3$ samples treated by solvent annealing. The dependence of the tensile fracture strength on grain size is shown in **Fig. 4**(e). They conclude that the development of coarse fractures in the perovskite layers is the major reason for the substantial drop in the PCE of the flexible PSCs, which was noticed through their SEM measurements after the end of the cyclic bending tensile test period. The in situ tensile testing used in their experiment clearly gives more realistic mechanical characteristics of perovskite materials, which are key indications of the mechanical dependability of flexible photovoltaic perovskite devices.

Nanoindentation Testing and Analysis

The quantitative assessment of the mechanical properties of a variety of hybrid organic-inorganic materials for solar cells has been facilitated by recent improvements in the nanoindentation technique. Nanoindentation is a widely used technique to investigate mechanical behavior of materials at various length scales. It can tell us a lot about the length scales at which the perovskite materials behave homogeneously and provide statistics far beyond what other mechanical tests can offer if mapping of the mechanical properties is applied. Nanoindentation provides a reliable way of probing the anisotropic mechanical behavior since the measured stiffness is strongly dependent on the elastic response along the indenter axis and only weakly affected transversely (Asif and Pethica, 2006; Jian *et al.*, 2013; Tan and Cheetham, 2011).

Author's personal copy

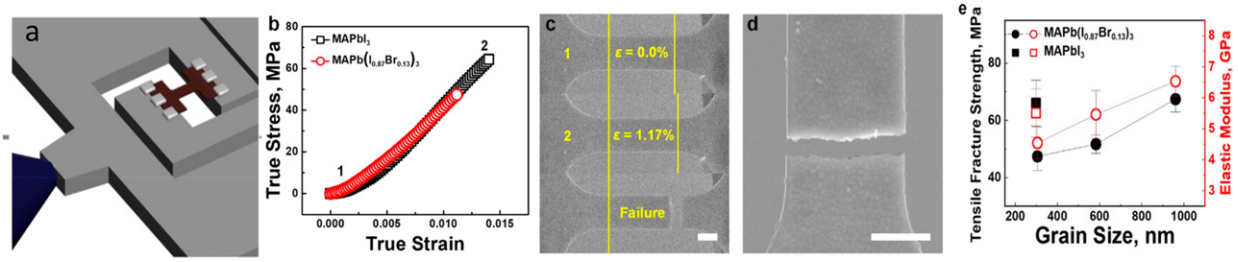

Fig. 4 (a) Schematics for sample preparation and in situ tensile testing of perovskite materials. (b) Typical tensile stress-strain curves for $MAPbI_3$ and $MAPb(I_{0.87}\ Br_{0.13})_3$ (c) Image correlation method for measuring tensile strain. (d) SEM image after tensile fracture showing intergranular fracture (e) Relation between mechanical properties and grain size. Reproduced from Ahn, S.-M., Jung, E.D., Kim, S.-H., *et al.*, 2019. Nanomechanical approach for flexibility of organic–inorganic hybrid perovskite solar cells. Nano Letters 19 (6), 3707–3715. With permission from American Chemical Society.

Nanoindentation technique has been used to obtain the mechanical properties of single crystal organic-inorganic halide perovskites $CH_3NH_3PbX_3$ (X = I, Br, and Cl) (Sun *et al.*, 2015). The stress states of $CH_3NH_3PbX_3$ (X = Cl, Br, I), as the indenter penetrates the sample surfaces, are usually depicted using typical load-displacement (P-h) curves to determine the elastic moduli. The residual depths after unloading have been shown to be high for Br and Cl based perovskites, showing that significant plastic deformation occurred under the Berkovich tip (Sun *et al.*, 2015). Based on this, they showed that Young's moduli of this family of perovskite lie in the range 10–20 GPa (Sun *et al.*, 2015) The mechanical properties of perovskites depend on the interaction of hydrogen bonding, the strength of Pb-halide bonds and the relative packing density.

The elasto-mechanical properties of single crystals of $APbX_3$ (A = Cs, CH_3NH_3; X = I, Br) perovskite have been shown by Yevgeny and Sidney have been related to variations in Pb-X bond and crystallographic orientation (Rakita *et al.*, 2015). The single crystals mechanical properties were probed by nano-indentation to measure their Young's modulus (E) and nano-hardness (H). The experimental results revealed that the Young's moduli of $CH_3NH_3PbI_3$, $CH_3NH_3PbBr_3$, and $CsPbBr_3$ are 14 GPa, 19.5, and 16 GPa, respectively, giving support to the theoretically predicted values. The elastic modulus of $CH_3NH_3PbI_3$ is lower compared to $CH_3NH_3PbBr_3$ which was attributed to variation in the strengths in Pb–X bond (Rakita *et al.*, 2015). Furthermore, the comparative result between $CH_3NH_3PbBr_3$ and $CsPbBr_3$ demonstrates that the organic group really stiffens the whole structure (higher elastic modulus). As this might be attributed to the variation in crystallographic orientation between the examined crystals, which is also in agreement with work of Sun *et al.* (2015), showing that the (100) orientation is stiffer than the (110) orientation in $CH_3NH_3PbBr_3$. As a result, the B–X bond appears to dominate the elastomechanical properties, with the presence of the A group decreasing the elastic coefficients of these large-cage perovskite-structured materials, thereby classifying HOIPs among the relevant material groups based on their elasto-mechanical properties.

The understanding of creep and stress relaxation in perovskite solar cells is also very crucial in reliability study. Reyes-Martinez *et al.* (2017) have used nanoindentation creep and stress relaxation to study the time- and rate-dependent mechanical properties of single crystal hybrid organic–inorganic perovskites (HOIPs) and an inorganic perovskite (IP) single. These include: methylammonium lead bromide ($CH_3NH_3PbBr_3$); methylammonium lead iodide ($CH_3NH_3PbI_3$), and an all-inorganic perovskite of cesium lead bromide ($CsPbBr_3$). Under the loading condition, the perovskite materials with low hardness crystals experience creep. In single crystal perovskites, dislocations occur during loading which is usually evident in the discontinuity of load–penetration curves (**Fig. 5** (a)) that result in pop-in events for the difference in elastic-to-plastic transitions. The typical SEM images of the single crystals of $CH_3NH_3PbBr_3$ and $CH_3NH_3PbI_3$ are shown in **Fig. 5**(b)-(c), respectively, for before and after indentation.

FCC crystals creep less during nanoindentation experiments due to dislocation movement along the axis of the indenter tip and a reduced number of accessible slip systems. Since nanoindentation initiates and propagates dislocations in crystalline materials, which can lead to plastic deformation [28], [32–34]. Perovskite single crystals exhibit significant creep deformation, stress relaxation, and noticeable rate-dependent mechanical behavior as compared to a KBr model ionic crystal. [28] As shown in **Fig. 6**, the variations in the creep and load relaxation curves obtained from the perovskite materials studied are attributable to dislocation events that occur during the nanoindentation experiments. The use of a rheological model to fit the experimental data for creep and relaxation behavior (**Fig. 6**(a)-(d)) have been used to provide insights into mechanical behavior of perovskite single crystal, thereby concluding that the implications of the results allow for the determination of both the elastic and viscous properties of the specific perovskite single crystals.

Most the current world record perovskite solar cells are made from formamidinium-based materials, making their mechanical properties to be so interesting. Sun *et al.* (2017) have investigated the anisotropic mechanical characteristics of formamidinium (FA) lead halide perovskites ($FAPbX_3$, X = Br or I) using nanoindentation. The nanoindentation experiment were carried out on the X-ray detachable facets of $FAPbI_3$ and $FAPbBr_3$ single crystals up to an indentation depth of 1000 nm. The hardness and Young's modulus of both $FAPbI_3$ and $FAPbBr_3$ are within the range of 0.36–0.45 GPa and 9–13 GPa, respectively (Sun *et al.*, 2017). The structures of FA are stiffest along inorganic Pb-X-Pb chains, which are oriented along $< 100 >$, compared with the mechanical properties methylammonium-based crystals. Two factors have found to greatly influence the mechanical behavior of the FA perovskite single crystals. These include presence of hydrogen bonding and the Pb-Br bond length.

Author's personal copy

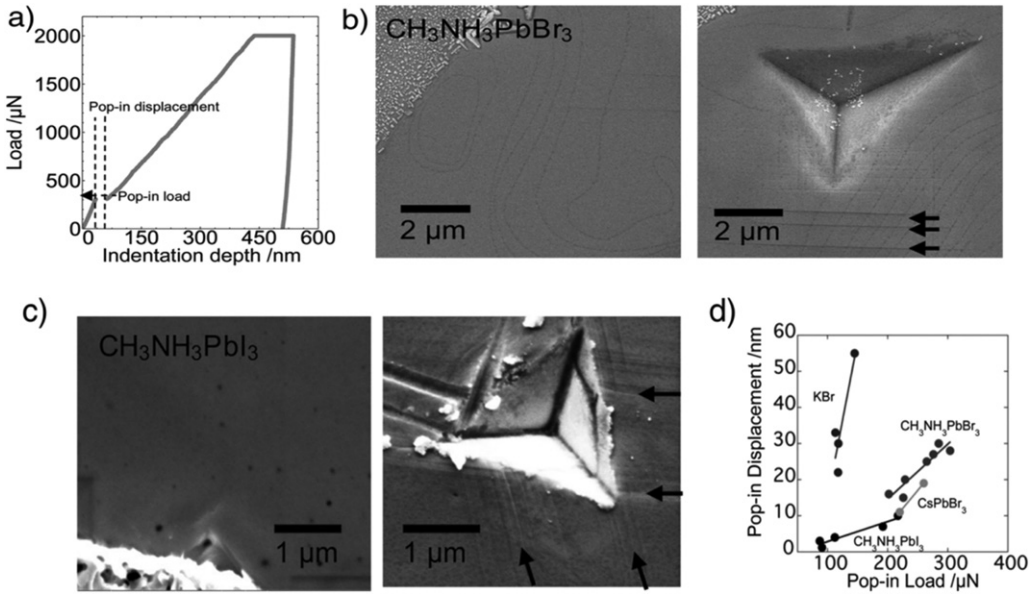

Fig. 5 (a) A pop-in event is captured during loading on a $CH_3NH_3PbI_3$ single crystal. The first pop-in event indicates the elastic-to-plastic transition. Scanning electron micrograph revealing slip bands (highlighted with arrows) on the surface of (b) $CH_3NH_3PbBr_3$ and (c) $CH_3NH_3PbI_3$ crystals as a result of plastic deformation during a nanoindentation experiment using a Berkovich indenter. Slip bands are expected from the activation of slip systems in a BCC crystal. (d) Measured pop-in displacement as a function of pop-in load for all single crystals tested. The inverse slope for each single crystal is related to the energy released during the initiation of slip dislocation. Reproduced from Reyes-Martinez, M.A., Abdelhady, A.L., Saidaminov, M.I., *et al.*, 2017. Time-dependent mechanical response of APbX3 (A = Cs, CH3NH3; X = I, Br) single crystals. Advanced Materials 29. With permission Wiley Publishing.

Bending Test

In solar cell reliability testing, it is important to relate the mechanical behavior of the cells to performance degradation. In conventional rigid silicon solar cells, three-point and four-point bending tests are used to check robustness in a way that simulate the reliability of solar cells under different bending deformations due to environmental conditions like snow and wind. In the case of flexible solar cells, bending test is used to certify the flexibility under deformation to different bending radii. It is, therefore, very important to look at the different mechanical bending tests in solar cells.

Three- and four-point bending tests are usually applied to rigid or brittle solar cell structures. The mechanical reliability of solar cells that are based on silicon can be studied using these testing techniques. Hence, the elastic modulus of bending and flexural stress/strain of the layered solar cells can be obtained. The interfacial robustness of the layered solar cells can also be verified using the three- or four-point bending test. Fig. 7(a)-(b) present the schematics of the three- and four-point bending tests, respectively. The flexural strength (σ) of solar cells and solar modules can be estimated using the simple forms of Eqs. (1) and (2) for three-point and four-point bending.

$$\sigma_{3-point} = \frac{3FL}{2wd^2} \tag{1}$$

and

$$\sigma_{4-point} = \frac{FL}{wd^2} \tag{2}$$

where F is the applied force, $w, Landd$ are the width, length and thickness of the sample.

Bending test in flexible and stretchable solar cell structures involves deformation of the layered structures around a roller with a well-defined radius. The bending strain of the layered structure can then be estimated. For simplicity, if we consider a bilayer structure of the solar cell that is bent around a roller (Fig. 7(c)-(d)) with radius, r, the bending strain (ε_b) of the bilayer structure of thickness, h, can be estimated using:

$$\varepsilon_b = \left(\frac{t_s + t_f}{2r}\right)\left[\frac{1 + 2\eta + \chi\eta^2}{(1+\eta)(1+\chi\eta)}\right] \tag{3}$$

Where $\eta = t_f/t_s, \chi = E_f/E_s$, t_s and t_f are the thicknesses of the substrate and the film, E_s and E_f are the Young's moduli of the substrate and the film, respectively. The level of strains in the flexible solar cell structure can be obtained and related to possible degradation.

Peel Test at Angle 90°

Solar cells are protected from degradation by encapsulating the cells between two layers of encapsulating materials with support from both sides. In silicon solar cells, a glass and a back sheet are usually used as supporting materials. For robustness

Author's personal copy

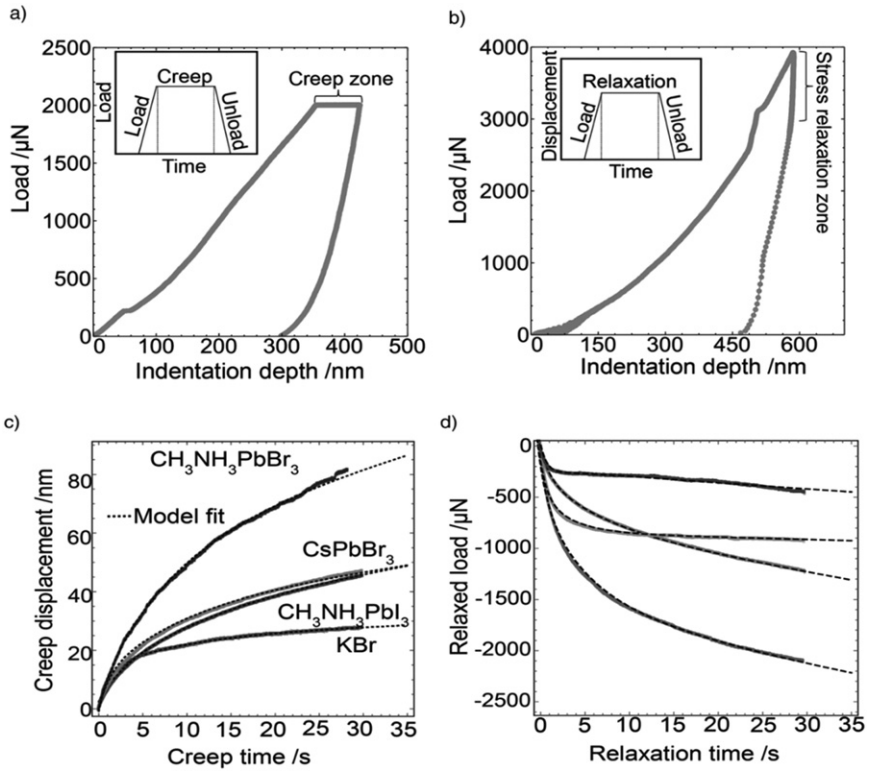

Fig. 6 a) Load–indentation depth curve for load-controlled nanoindentation experiment on a $CH_3NH_3PbI_3$ single crystal. The load function in the inset displays loading, constant-load (creep) and unloading with time. The ramp time to maximum load was $t_R = 20$ s and the maximum load was held at $P_{max} = 2000$ μN for 30 s in all creep experiments. b) Representative load–indentation depth curve for displacement-controlled nanoindentation experiment on the same CH3NH3PbI3 single crystal. The displacement function in the inset displays loading, constant displacement holding (stress relaxation) and unloading with time. The ramp time to maximum displacement was $t_R = 20$ s and the maximum displacement was held at $d_{max} = 600$ nm for 30 s in all stress relaxation experiments. c) Creep displacement curves and d) load relaxation curves for the four single crystals tested. Bands represent the standard error extracted from three independent measurements on each single crystal. The fit of our model (dotted line) captures the behavior of all the single crystals tested in both creep and stress relaxation experiment. Reproduced from Reyes-Martinez, M.A., Abdelhady, A.L., Saidaminov, M.I., *et al.*, 2017. Time-dependent mechanical response of APbX3 (A = Cs, CH3NH3; X = I, Br) single crystals. Advanced Materials 29. With permission Wiley Publishing.

and long-lasting cells, it is very important that the interfacial adhesion along glass-encapsulant, encapsulant-encapsulant, and encapsulant-back sheet interfaces are strong at the edges to stop percolation of moisture into the cells. One of the ways of testing the interfacial mechanical property is peel test. It basically assesses the quality of bond between two different layers. Fig. 7(e) presents the schematics of a typical peel test. A layer is peeled off at an angle to measure the load-extension curve that is associated with the peel off. One of the easy-to-configure is peel test at angle 90°, which has been used for testing the interfacial mechanical properties in silicon cells and module reliability testing.

For a typical load-extension curve result from a typical peel test at angle 90° (Fig. 7(f)), a peak load initiates crack along the interface before dropping to a constant load that is required to continue peeling a layer off the other. The load per unit width can therefore be estimated from the flat portion (constant load region) of the load-extension curve. The peak load that initiates the interfacial failure can also be used to characterize degradation due to environmental effects.

Interfacial Fracture in Layered Solar Cell Structures

In solar cell structures, the integrity of interfaces between layers are very key to performance, robustness and lifespan of devices since the electron-hole pairs are usually transported across these interfaces. Many solar cell devices (from inorganic to organic structures) fail due to interfacial defects and fracture that are initiated by stresses within the layers or surface of the layers. These stresses can be thermally induced during service conditions. They can also be initiated by chemical reactions between layers or induced by physical deformation due to environmental effects. This section shows how to measure and characterize the interfacial mechanical fracture in layered solar cell structures along with the design of robust structures that have strong interfacial interactions between layers.

Author's personal copy

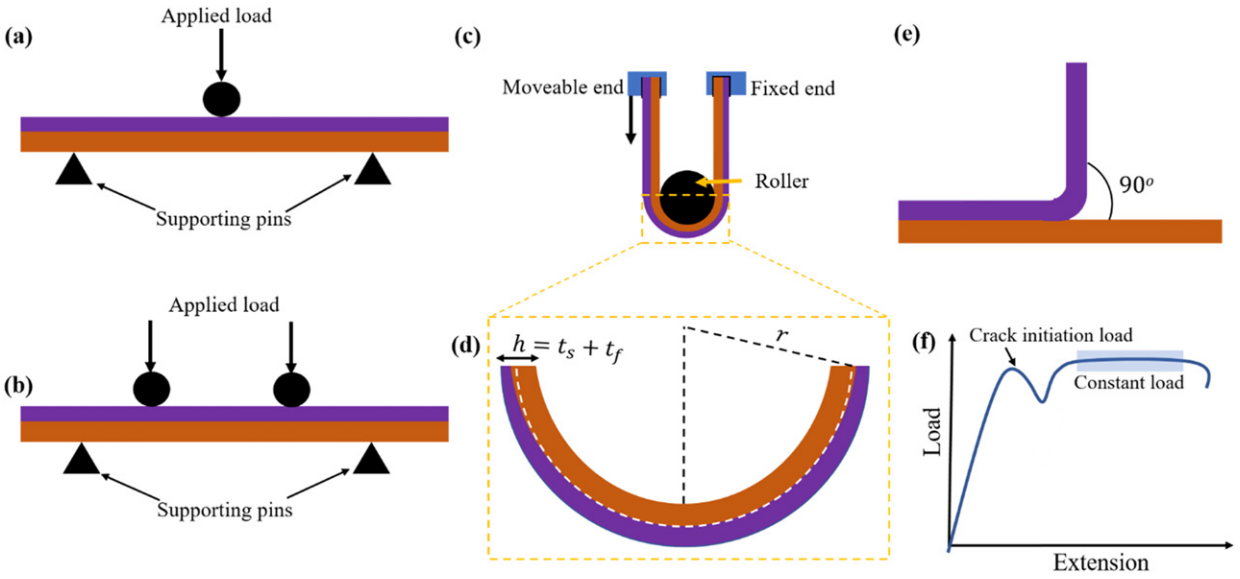

Fig. 7 Schematics of various testing methods in testing mechanical properties of solar cells: (a) Three-point bending test, (b) Four-point bending test, (c-d) Bending test for flexible solar cells using a roller to define the bending radius, (e) Peel test and (f) Typical load-extension curve from a peel test at angle 90°.

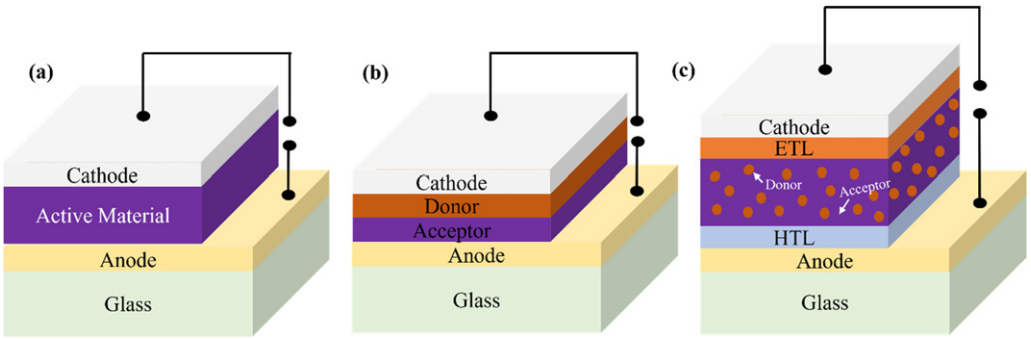

Fig. 8 Various architectures of Organic solar cells: (a) Single layer OSC, (b) Bilayer OSC, and (c) Bulk heterojunction OSC.

Designs of Emerging Solar Cells

Before showing some of interfacial fracture measurement techniques in some few classes of emerging solar cells, it will be interesting to quickly describe the architecture of organic bulk heterojunction solar cells (OSCs) and hybrid organic-inorganic perovskite solar cells (PSCs) which are two emerging cost-effective photovoltaic devices.

Before the introduction of bulk heterojunction OSCs, the architectures of OSCs comprise of a single organic photoactive polymer sandwiched between two electrodes of different work functions (**Fig. 8**(a)). In this type of single-layer organic photovoltaics (OPVs), the built-in potential is achieved either from the difference in electrodes work function or from a Schottky-type potential barrier at one of the metal or the organic interfaces (Merritt and Hovel, 1976; Popovic and Loutfy, 1981; Tang and AlBrecht, 2008) The properties of the PV depend on the work function of the electrodes. Hence, they suffer from large series resistance associated with the insulating nature of the organic layer which results in poor fill factor (FF). They also experience recombination of holes and electrons due to insufficient internal electric field generated for dissociation of excitons, resulting in low quantum efficiencies (<1%) and low power conversion efficiencies PCE of (<0.1%) (Weinberger *et al.*, 1982).

Bi-layered OSC structures were explored in 1986 (Tang, 1986) by Tang *et al.* The bi-layer structure consists of an electron donor and an electron acceptor as the photoactive layers (**Fig. 8**(b)). The donor and acceptor material have different electron affinity and ionization energies, hence electrostatic forces are generated at the interfaces of the two materials. The electron acceptor has a higher electron affinity and greater ionization energy, while the electron donor has a lower electron affinity and lower ionization energy.

However, the interface between the two thin organic materials is important in determining its photovoltaic properties. The interface between the two organic material is mainly responsible for the photogeneration of charges. The two photoactive materials are chosen carefully such that the local electric fields around the interface are strong enough to split excitons that are created much more effectively. This helps overcome the serious limitation of the single layer photovoltaic cells, and providing the bi-layer OSCs with a considerably higher FF, and a power conversion efficiency of 1% (Tang, 1986).

Author's personal copy

In the case of the bulk heterojunction OSCs, (Akogwu *et al.*, 2011; Jae *et al.*, 2008; Kim *et al.*, 2011; Lipomi *et al.*, 2011; Venkateswararao *et al.*, 2018) the electron donor and electron acceptor materials are intimately mixed in a bulk volume to form the photoactive layer (as shown in **Fig. 11**(c)). More excitons, typically having short lifetimes can reach the donor-acceptor interface and get dissociated before they are able to recombine due to a large interfacial area, leading to a more efficient transport of charges across the active layers. The essence of the bulk heterojunction is to have each donor-acceptor interface within a distance that is less than the exciton diffusion length. The efficiency of BHJ OSC relies on the ability of the photogenerated excitons to reach the heterojunction between the donor and acceptor, generating free charge carriers, combined with the ability of these free charge carriers to escape to the electrodes.

The photoactive bulk heterojunction is made of a blend of polymeric materials which can be fabricated on rigid or flexible/stretchable substrate. The conventional bulk heterojunction structure is a blend of poly(3-hexyl)thiophene (P3HT) and [6,6]-phenyl-C61-butyric acid methyl ester (PCBM). Other photoactive polymeric materials have been used to improve both the optoelectronic and mechanical properties of OSCs. The anodes are made of transparent conducting oxides (TCO) which include rigid indium tin oxide (ITO), zinc oxide and some other conducting oxide that very transparent. Most of these TCOs are very brittle with $\sim$ 1% strain to failure. In most cases, an interface modifier of (poly(3,4-ethylenedioxythiophene) poly(styrene-sulfonate) (PEDOT:PSS) is used between the anodic layer and the photoactive bulk heterojunction layer. A layer of Calcium or lithium fluoride (LiF) is sometimes deposited onto the photoactive layer to protect and passivate the surface from moisture before depositing cathode material for complete cells (as shown in **Fig. 8**(c)). Except for the cathode that usually require thermal evaporation, most of the layers in the above designed architectures are deposited by spin coating techniques.

The architectures of perovskite solar cells are like those of the OSC structures. The difference between both types of photovoltaic devices is the nature intrinsic properties of photoactive layer. On like the organic semiconductor in OSCs, the photoactive layer in perovskite solar cells (PSCs) is made of metal-halide perovskite photoactive structure PSCs consists of primary active layers of metal-halide perovskite. The active layer is usually sandwiched between an electron transport layer (ETL) and a hole transport layer (HTL), as shown in **Fig. 9**. The layered PSC structure can be planar (**Fig. 9**(a)), mesoscopic (**Fig. 9**(b)) and inverted (**Fig. 9**(c)).

In all these emerging solar cell structures, the understanding of interfacial fracture toughness is crucial for enhanced performance and reliability. Several techniques have been used to measure interfacial fracture toughness with a single mixed mode such as micro-scratch, peel, bulge (Modi and Sitaraman, 2004), AFM (Tong *et al.*, 2009; Yu *et al.*, 2014) and double cantilever beam (DCB) (Rolston *et al.*, 2016). The interfacial fracture toughness can also be measure using variety of mode mixity to capture large energy release rates that is typical for thin film interfaces, These include Brazil disk test (Tong *et al.*, 2014) and modified decohesion test (MDT) (Modi and Sitaraman, 2004). Despite that power conversion efficiency (PCE) of PSCs has reached world record of over 25% (NREL, 2020), the values of adhesive and cohesive fracture resistance, G_c is below 1.5 J/m^2 for solution-processed devices. However, the typical fracture energy of OSCs is between $\sim$5–15 J/m^2 despite that PCE is 17.62% for single junction structure (Zhu *et al.*, 2021) which is lower than PSCs. The correlation between mechanical integrity and power conversion efficiency (PCE) degradation rates have been shown (Rolston *et al.*, 2016) in a way that explain the instability of solar devices for crystalline silicon (c-Si), copper Indium gallium selenide (CIGS), organic photovoltaics, and perovskite solar cells. Both OSCs and PSCs have relatively low cohesion energy and fast degradation rates relates compared to silicon-based solar cells. Therefore, efforts to enhance the reliability of OSCs and PSCs is generally considered very important as they emerge as future solar cells that be made in rigid, flexible and stretchable forms.

Interfacial Fracture in Layered Perovskite Solar cells (PSCs)

Interfacial adhesive fracture of stressed thin films often occurred in solar cell devices during operation and handling. The failure is often due to the weak adhesion between interfaces in the layered structures. Generally, films will adhere to the substrate upon deposition, though delamination may occur at any time due to many factors. In solar cells, residual stress can induced cracking (Wang *et al.*, 2019a) which can grow over time, thermal expansion mismatch stresses between different layers, defect formation can occur during grain coalescence/growth, fabrication, installation, and operation (Francis *et al.*, 2002). Furthermore, additional mechanical stresses during bending of flexible solar cells (Dupont *et al.*, 2012) and stretching of stretchable solar cells are also factors that accelerate delamination-induced phenomena along the interfaces with poor adhesion. Although the delamination

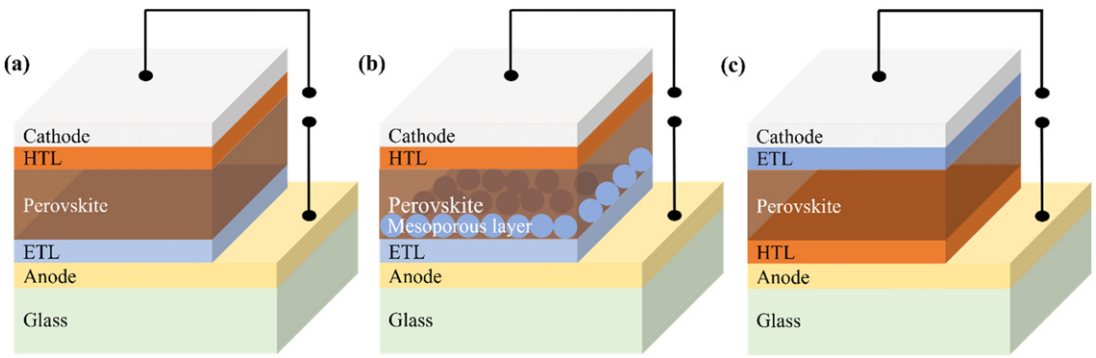

Fig. 9 Various architecture of perovskite solar cells: (a) Planar structure, (b) mesoscopic structure, and (c) Inverted structure.

Author's personal copy

failure of solar devices is affected by many factors, knowledge of the interfacial fracture toughness G_c is important to predict interfacial robustness and mechanical reliability of multilayered devices.

PSCs are made of multiple functional layers of materials with different thermal and mechanical properties. Multilayered perovskite solar cells (PSCs) consist of four different main interfaces in the structures, such as interfaces of fluorine-doped tin oxide (FTO)/electron-transport layer (ETL), ETL/perovskite, perovskite/hole-transport layer (HTL), and HTL/metal. In PSCs structures, delamination between layers is an important issue at interface of perovskite and adjacent layers in the structures, leading to loss of device performance due to defect-induced reduction in the open circuit voltage. Hence, interfacial detachment has been studied as one of potential degradation pathways when solar devices is exposed to air and moisture. In solution-processed of PSCs, interfaces between organic-inorganic perovskite and the adjacent layers are observed to be susceptible to delamination, failing at fracture resistance energy of less than 1.5 J/m^2 measured by Double cantilever beam (DCB) testing (Dai *et al.*, 2021). Organic charge transport layers are determined to have the weakest fracture energy where the mechanical failure initiates in solar devices (Rolston *et al.*, 2016).

Strong adhesion between perovskite and hole transport layer (HTL) are required for highly efficient PSCs structures. However, a weak interfaces in device structures can initiate interfacial detachment of layer (Lee *et al.*, 2017). Delamination of protective HTL from perovskite surface would accelerate the perovskite decomposition by directly exposing perovskite to the atmosphere (Yun *et al.*, 2015). Interface between perovskites and widely used hole transport layer SpiroOMeTAD- 2,2′,7,7′-tetrakis-(N, N-di-4-methoxyphenylamino) − 9,9′-spirobifluorene) was found to have lowest interfacial fracture energy. The interfacial fracture energies of 0.65 ± 0.21 J/m^2 and 1.61 ± 0.3 J/m^2 have been shown for interface between perovskite and SpiroOMeTAD for with and without the ion additive lithium bis (trifluoromethylsulfonyl)imide (Li-TFSI) in the SpiroOMeTAD, respectively. Interface between perovskite and SpiroOMeTAD is prone to moisture-induced degradation attributing to interfacial delamination at high humidity condition, where the ion additives accelerated the degradation phenomena by attracting more water molecules to the interfaces (Lee *et al.*, 2017). Thermal energy has also been observed to act as the driving force for ion migration of perovskite elements, where lead (Pb) and iodine (I) elements in $MAPbI_3$ layer diffuse to SpiroOMeTAD HTL layer after heat treatment from 50° to 250°C. Furthermore, in the case of ETL/perovskite interfaces, interfacial delamination has been observed between perovskite and compact titanium dioxide ($cTiO_2$) upon illumination as there is an inherent collective migration of interstitial ions/ion vacancies causing buckling in $MAPbI_3$ structure (Soufiani *et al.*, 2017).

Improving the reliability of multilayered PSC structures is generally challenging as active layer has inherent poor mechanical properties. For a single crystal perovskite, the Young's modulus (E) of ~ 17.8 GPa, low hardness (H) ~ 0.6 GPa and low toughness, (G_c) ~ 2.7 J/m^2 have been reported for methylammonium lead iodide using nanoindentation technique (Ramirez *et al.*, 2018). However, there are attempts to enhance interfacial fracture resistance of multilayered PSCs structures. There have been studies to strategize the fracture toughness, G_c, of the weakest interface in PSCs by adding interfacial layers (Dai *et al.*, 2021; Li *et al.*, 2014; Yun *et al.*, 2015), scaffolding, interpenetrating interfaces (Dong *et al.*, 2021b), introducing additives (Gutwald *et al.*, 2020), and grain coarsening (Dai *et al.*, 2020). Dai *et al.* (2021) proposed interfacial toughening at interfaces between hybrid organic-inorganic perovskite layer and SnO_2 electron transport layer (ETL) by introducing "molecular glue" at the interface used iodine-terminated self-assembled monolayer (I-SAM), contributing to increased PCE to 21.44% and improved stability up to ~4000 h. The introduction of I-SAM has improved the mechanical integrity between SnO_2/perovskite interfacial contact by decreasing the migration-induced formation of interfacial voids that are likely be a center of photocarrier recombination and interfacial cracks (Bi *et al.*, 2018; Dai *et al.*, 2021).

In the case of perovskite/HTL interfaces, adhesion enhancement has also been done by introducing polyethylene-imine (PEI) compatibilizer at the interface, which increased interfacial fracture energy from G_c of 0.65 ± 0.21 J/m^2 without PEI to G_c of 1.44 ± 0.30 J/m^2 with PEI interlayer (Yun *et al.*, 2015). Moreover, organic cation additives of 5-aminovaleric acid (5-AVA) have been found to effectively reinforce $MAPbI_3$ perovskite in increasing the fracture resistance from 0.53 J/m^2 to 6.04 J/m^2 by increasing the plasticity and crack deflection around perovskite grain boundaries (Gutwald *et al.*, 2020). Lastly, an interpenetrating perovskite/electron transport layer interface, by reacting FAI-incorporated SnO_2 ETL layer and PbI_2-excess perovskite layer, is also incorporated in PSCs structures for not only prevent ionic or molecule diffusion but also decrease the susceptibility for interfacial fracture, leading to PCE up to 22.2% and 20.1% for rigid and flexible substrates (Dong *et al.*, 2021b).

Interfacial Fracture in Layered Organic Solar Cells (OSCs)

Analogous to perovskite solar cells that comprise a multilayer structures, layered organic electronic devices also experience delamination between layers when charge transport occurs through the layers under continuous illumination (Tong *et al.*, 2009). In addition, residual and applied stress would accelerate the cohesive cracks, leading to interfacial debonding and deformation within layers in organic photovoltaic devices (Dupont *et al.*, 2012). Furthermore, solvent evaporation, chemical reaction, and phase separation of polymers during device processing play roles in different shrinkage strains and associated stresses (Francis *et al.*, 2002). Those mechanical and chemical factors contribute to the reduce in adhesion in layered OSCs. Such loss of adhesion, particularly at electrical contacts, would promote the exciton recombination and series resistance, leading to reduction in fill factor of devices (Yongjin, 2013). Therefore, interfacial fracture toughness of OSCs is an important metric to design robust and long-term reliable organic solar cells in the future.

Recent studies have investigated adhesion energies of each layer that relevant to standard organic solar cell structures by utilizing an AFM technique. Localized nanoscale adhesion between asperities on the surface that are relevant to organic solar cells structures (**Fig. 8**(c)) on rigid (Tong *et al.*, 2009) and flexible substrates is measured (Yu *et al.*, 2014). By interacting two interest surfaces and incorporating the measured adhesion force to adhesion energy model, interfaces between photoactive region poly(3-hexyl)thiophene:[6,6]-phenyl-C61-butyric acid methyl ester (P3HT:PCBM) and hole transporting layer poly(3,4-ethylenedioxythiophene) poly

Author's personal copy

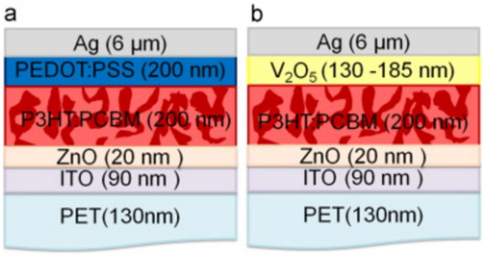

Fig. 10 Device structure of inverted OSCs with hole transport layers of (a) PEDOT:PSS and (b) V_2O_5. Reprinted from Dupont, S.R., Oliver, M., Krebs, F. C., *et al.*, 2012. Interlayer adhesion in roll-to-roll processed flexible inverted polymer solar cells. Solar Energy Materials and Solar Cells 97. Elsevier.

(styrene-sulfonate) (PEDOT:PSS) and interfaces between PEDOT:PSS and ITO substrate are mechanically the strongest, with both adhesion energy of $\sim 40 \pm 4$ J/m^2, compared to other interfaces. The layer of P3HT:PCBM adhere strongly to PEDOT:PSS would be due to the physical intermixing of P3HT and PSS. Fullerene derivative PCBM with dense delocalized electron would also contribute in enhancing interactions between P3HT:PCBM and other materials (Tong *et al.*, 2009; Yu *et al.*, 2014).

Furthermore, in the advanced applications of organic electronics to stretchable and bendable organic solar cells, interfacial robustness is very important for prediction of failure over multidimensional stress states. Mode mixity dependence of interfacial fracture toughness in organic solar cells structures has also been studied using Brazil disk specimen (CCBD) fracture test that can be oriented at a particular angle to measure the interfacial fracture toughness over broad range of mode mixities, ranging from pure opening mode I and pure in-plane shear mode II. Interface between quartz and PEDOT anode exhibit 0.97 ± 0.16 J/m^2 and the fracture toughness increases with increasing mode mixity (Tong *et al.*, 2014).

Adhesive and cohesive behavior of bi-material layers and thin films are important properties for producing long-term reliable multilayered electronic devices (Brand *et al.*, 2012). Therefore, there have been some efforts to enhance the adhesive and cohesive properties of layer and interfaces in OSCs, such as introducing interlayer (Nehm *et al.*, 2017; Wang *et al.*, 2011), optimizing annealing temperature and time, increasing P3HT molecular weight, and adjusting active layer thickness (Bruner and Dauskardt, 2014), and replacing the hole transporting layer (Dupont *et al.*, 2012). In terms of introducing interlayer in OSCs, Nehm *et al.* (2017) have observed that there are reduced extrinsic degradation for OSCs with MoO_3/Cr/Al compared to the devices with standard Al electrode, due to enhanced cathode adhesion from additional interlayers. Oh *et al.* (2011) have also inserted a controlled thickness of P3HT between P3HT:PCBM/PEDOT:PSS interface to modify the surface property from hydrophilic to hydrophobic. Desirable vertical phase separation is achieved by incorporating P3HT at that interface, contributing to higher photogenerated carrier and improved power conversion efficiency (44%) compared to the reference OSCs. Therefore, sufficient toughening of interfaces between layers in electronic devices is needed to achieve long-term reliable devices.

In flexible inverted P3HT:PCBM bulk heterojunction (BHJ) cells in **Fig. 10**(a), interfaces between blend active layer and adjoining interfaces are mechanically weakest, causing loss in device performance. Using DCB testing, fracture resistance at interfaces of P3HT:PCBM/PEDOT:PSS in inverted OSCs has the weakest interfaces varies from 1.6 J/m^2 to 0.1 J/m^2, depending of different P3HT:PCBM compositions (Dupont *et al.*, 2012) P3HT- rich BHJ layer produce stronger interface to PEDOT:PSS compared to PCBM-rich BHJ layer, although PCBM is more hydrophobic (Oh *et al.*, 2011). Moreover, thermal post-annealing temperature and time also improved fracture energy as PCBM diffuse away from the interface (Dupont *et al.*, 2012). Finally, replacing HTL replacement has also been explored to increase the interfacial fracture energy in inverted device structures via roll-to-roll processing. Metal oxide V_2O_5 is chosen to replace PEDOT:PSS HTL in **Fig. 10**(b) resulting doubled increment of fracture energy due to stronger molecular interactions that involves the chemical bond formation such as covalent, ionic and bipolar bonds.

Interfacial Fracture in Lamination of Solar Cells

Lamination of layered materials has been considered as a quick fabrication process for emerging organic solar cells and perovskite solar cells (Oyewole *et al.*, 2015). Different layers of these electronic structures can be processed using lamination technique. Lee *et al.* (2010) have shown the lamination of top electrode in organic photovoltaic cells that are transparent. A single step lamination approach has also been demonstrated by Huang *et al.* (2006) for semitransparent polymer solar cells. Low temperature lamination processes have also been used by Guo *et al.* (2001). Lamination technique has also been used for integrating Li-ion battery materials onto a single sheet of paper. (Hu *et al.*, 2010; Oyewole *et al.*, 2015) have used a combination of experimental, computational and analytical approaches to provide general insights for the design of lamination processes of organic photovoltaic cells (OPVs). This section explores the design of lamination processes that are relevant OPVs using the understanding of mechanical interfacial fracture.

Fracture mechanics model for lamination of solar cells

During the lamination of a thin layer from a stamp, two stages are generally involved - pre-lamination and lift-off stages/processes. The pre-lamination is the process of applying a compressive force to the stamp to make a considerably good contact with the substrate while lift-off process is the gently removal of the stamp from the laminated layer. Ideally, it expected that the laminated film adheres to the substrate while the interface between the stamp and the laminated fractures during the lift-off. However, the

Author's personal copy

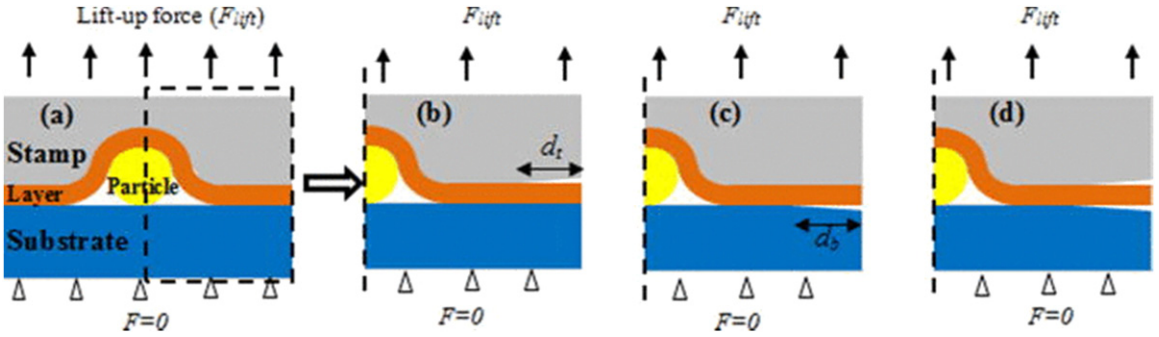

Fig. 11 (a) Schematics of micro scale models of interfacial fracture during the lift-off process of the lamination: (a) model of the lift-off process after the press down of the layer on the substrate, (b) axisymmetric model of successful lift-off, (c) axisymmetric model of unsuccessful lift-off, and (d) axisymmetric model of partial interfacial fracture. Reproduced from Oyewole, O.K., Yu, D., Du, J., *et al.*, 2015. Lamination of organic solar cells and organic light emitting devices: Models and experiments. Journal of Applied Physics 118 (7). With permission from AIP Publishing.

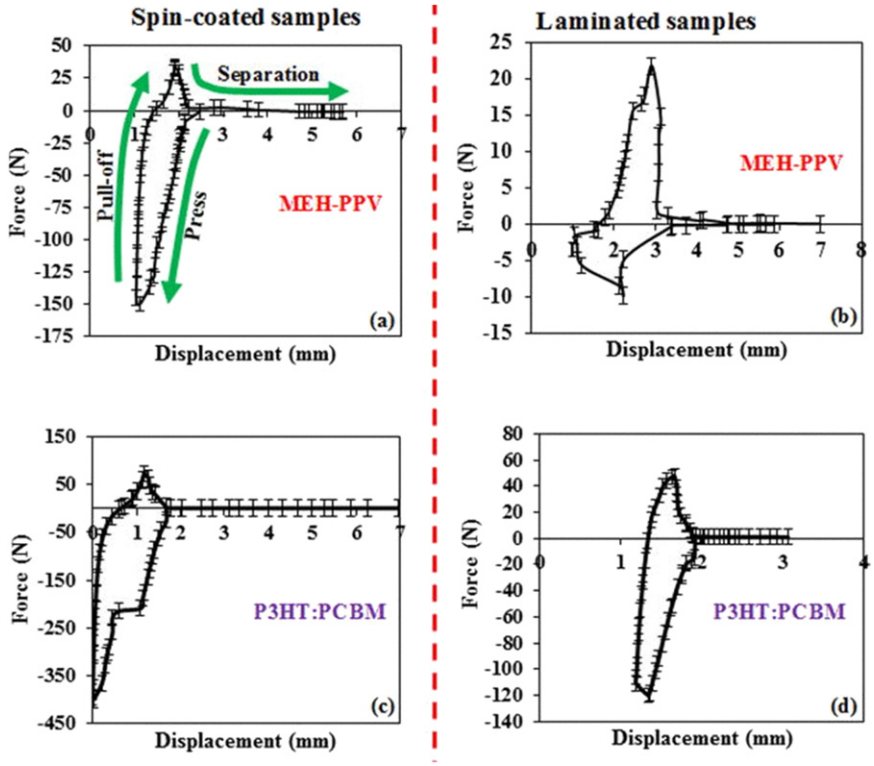

Fig. 12 (a) Force-displacement curves of pull-off of (a) spin-coated MEH-PPV, (b) spin-coated P3HT:PCBM, (c) laminated MEH-PPV, and (d) laminated P3HT:PCBM. Reproduced from Oyewole, O.K., Yu, D., Du, J., *et al.*, 2015. Lamination of organic solar cells and organic light emitting devices: Models and experiments. Journal of Applied Physics 118 (7). With permission from AIP Publishing.

case is difference especially when there are unforeseen defects along the interface of interest. The defects can be initiated by clean room particles that are sandwiched along the interface (Cao *et al.*, 2005) which can therefore cause stress concentrations that can ultimately lead to interfacial crack growth and fracture in the layered structure.

It is important to note that three possible scenarios can take place during the lift-off of the lamination process. These include: steady interfacial delamination between the laminated layer and substrate (called unsuccessful lamination); steady interfacial delamination between the stamp and laminated layer (called successful lamination), and there can also be a possible simultaneous delamination in interfaces of the transferred layer/substrate, and the stamp/transferred layer – partial lamination. The model of the fracture during in lift-off process has been shown by Oyewole *et al.* (2015). In a scenario where there is a particle between the layered interfaces during pre-lamination, edge cracks are also idealized between the transferred layer and stamp and/or between transferred layer and substrate (**Fig. 11**). The energy release rates at the tips of the edge cracks are measures of the crack driving force (Oyewole *et al.*, 2015). The relationship between the energy release rate and the interfacial cracks is given by Oyewole *et al.* (2015)

Author's personal copy

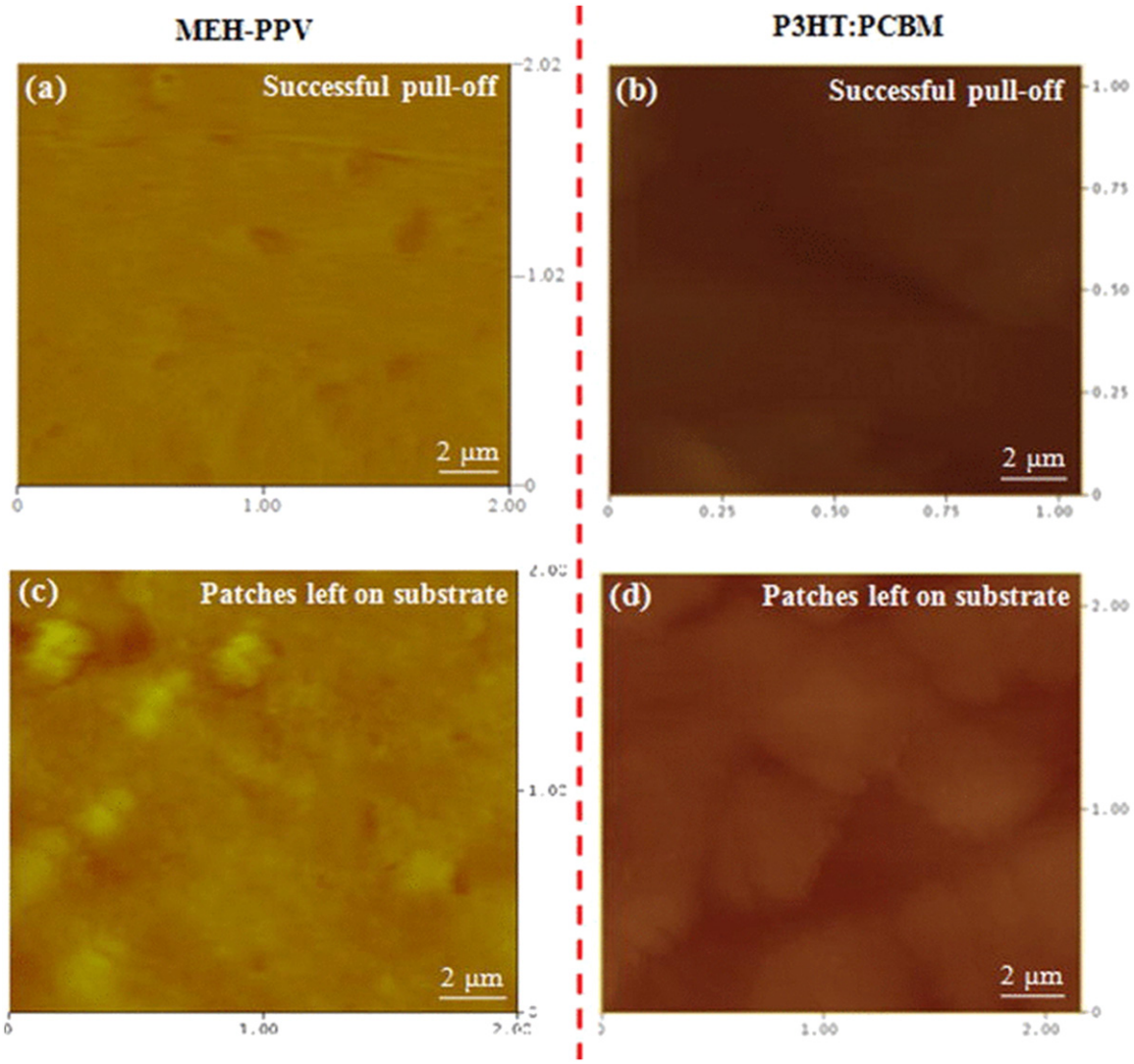

Fig. 13 Samples of the AFM images of substrates after pull-off of active layers, MEH-PPV, and P3HT:PCBM for (a) and (b) successful pull-off, (c) and (d) pull-off with remnants left on the substrates. Reproduced from Oyewole, O.K., Yu, D., Du, J., *et al.*, 2015. Lamination of organic solar cells and organic light emitting devices: Models and experiments. Journal of Applied Physics 118 (7). With permission from AIP Publishing.

$$G = f\left(\frac{\overline{E}_s}{\overline{E}_f}, \frac{t_s}{t_f}, \frac{d_b}{t_f}, \frac{d_t}{t_f}\right)\frac{\sigma^2 t_f}{\overline{E}_f} \tag{4}$$

where $\overline{E}_f = E_f/(1-\nu^2)$ is the plane strain elastic moduli of the film, $\overline{E}_s = E_s/(1-\nu^2)$ is the plane strain elastic moduli of the substrate, d_t is the length of top interfacial crack, d_b is the length of the bottom interfacial crack, t_f is the thickness of the film, t_s is the thickness of the substrate and σ is the lift-up stress. Eq. (4) can also be written as:

$$G = f\left(\frac{\overline{E}_s}{\overline{E}_f}, \frac{t_s}{t_f}, \frac{d_b}{t_f}, \frac{d_t}{t_f}\right)\frac{F_{Lift-off}^2 t_f}{w^2 L^2 \overline{E}_f} \tag{5}$$

where $\sigma = F_{Lift-off}/wL$, w and $L$are the width and length of the structure, respectively.

As shown in **Fig. 16**, two interfaces (the top and the bottom) are the possible interfaces during lamination process. The energy release rates (G_t) and (G_b) at the tips of the edge crack at the top existing edge cracks of lengths, d_t and d_b , at the top and bottom interfaces, the energy release rate at the tip of the edge crack at the top interface is denoted as G_t, while the energy release rate.

As shown in **Fig. 11**, two different interfaces (the top and the bottom) are possible during the lamination process. Any or both interfaces can fracture during the lift-off process. The energy release rates, (G_t) and (G_b), at the tips of the top and bottom cracks can be related to explain the success of lamination process in form of differentials of the driving forces of the propagating cracks along the interfaces. (Tucker *et al.*, 2009) At a critical condition, the differential of the interfacial energy release rates (G_t^c and G_b^c) of the edge cracks at the top and bottom interfaces can be expressed as (Tucker *et al.*, 2009)

Author's personal copy

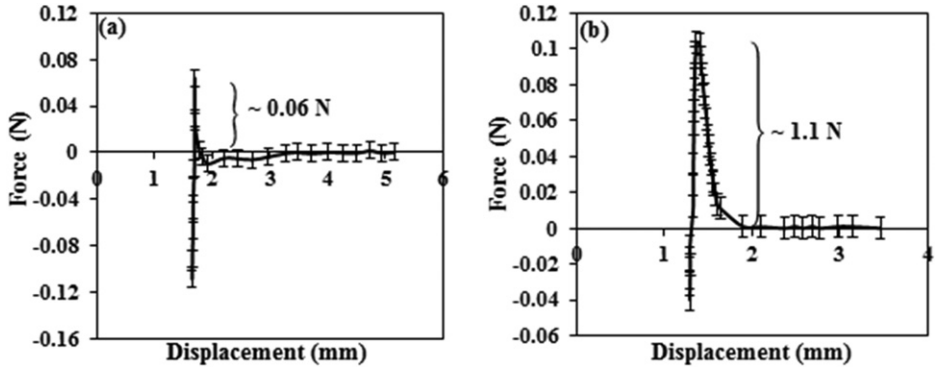

Fig. 14 Force-displacement curves of pre-lamination of (a) P3HT:PCBM and (b) MEH-PPV on PEDOT:PPS-coated glass. (a) The peaks represent the interfacial adhesion forces along PDMS/ MEH-PPV and PDMS/P3HT:PCBM interfaces during lift-off of the stamp from P3HT:PCBM and MEH-PPV. Reproduced from Oyewole, O.K., Yu, D., Du, J., *et al.*, 2015. Lamination of organic solar cells and organic light emitting devices: Models and experiments. Journal of Applied Physics 118 (7). With permission from AIP Publishing.

$$\frac{G_t}{G_b} = \frac{G_t^c}{G_b^c} \tag{6}$$

The interfacial crack will propagate along the top interface, if $G_t/G_b > G_t^c/G_b^c$, leading ultimately to delamination of the stamp from the transferred layer for a successful lamination process. However, if $G_t/G_b < G_t^c/G_b^c$, the crack propagates along the bottom interface, causing delamination of the laminated layer from the substrate. In this case, the lamination is unsuccessful.

As a demonstration of the effectiveness of the lamination techniques, organic materials have been laminated on glass using a PDMS stamp. Fig. 12(a)-(d) present the results of pull-off tests, comparing laminated and spin-coated P3HT:PCBM and MEH:PPV active layers. The peaks of the force-displacement curves represent the interfacial adhesion force between the active layers and the PEDOT:PSS-coated substrates. The adhesion forces of the spin coated and laminated samples are comparable for both MEH:PPV/ PEDOT:PSS (Fig. 12(a)-(b)) and P3HT:PCBM/PEDOT bottom interfaces (Fig. 12(c)-(d)) active materials. Fig. 13 showed evidence of scenarios when the lamination is successful or not. In the case of successful lamination, no remnant of the pulled-off MEH-PPV and P3HT:PCBM were observed on the substrates after pull-off (Fig. 13(a)-(b)) while patches of the laminated MEH-PPV and P3HT:PCBM layers are evident in the case where the layers are not fully pulled off from the substrate (Fig. 13(c)-(d)).

In the case of the top interfaces between the PDMS and the active materials, the adhesion forces are very low compared to the bottom interfaces of interest. Fig. 14(a)-(b) presents the experimentally measured adhesion forces at the interfaces of Stamp/P3HT:PCBM (Fig. 14(a)) and Stamp/MEH:PPV (Fig. 14(b)). High adhesion forces at the bottom interfaces and low forces at the top interfaces suggests that the stamps can be removed easily from the laminated active layers, without damaging the interfaces between the active layers and PEDOT:PSS-coated glass for successful lamination.

It is important to note that interfacial cracks can kink in- and-out of interfaces, which can lead to patches of partial interfacial separation during material during pull-off. This can occur due to micro-void nucleation around inclusions and interfacial impurities link with dominant interfacial cracks in ways that promote the extension of interfacial cracks into adjacent layers. Hence, the crack can kink in-and-out of interfaces depending on the distribution of the inclusion/impurities that include the formation of voids that link up with the propagating cracks.

Since the presence of inclusion/impurities is very critical to device interfacial robustness in emerging solar cells, delamination of the stamp from the laminated layer as well as the delamination of the laminated layer from the substrate, during the lift-off process, becomes more interesting at the micron-scale. By considering the voids that are produced as a result of the wrapping of the thin films around micro-particles that are trapped between the substrates and laminated layers (Fig. 11), typical results the interfacial fracture that occurs during the lift process is presented in Fig. 15 for different lengths of the void created by the impurities. For the lamination of active layers, the initial energy release rate at the top interface was initially at the maximum value before it decreased to zero, while the energy release rate at the bottom interface (that was initially at zero) increased, as the energy release rate at the top interface decreased. Meanwhile, the energy release rates of the top and bottom cracks decreased, as the length of the crack (void) created by particle increased (Fig. 15(a)-(d)). It can also be seen in Fig. 15 that the energy release rates (G_{void}) at the tips of the cracks, which were created by the trapped impurities, increased with increasing size of the impurity and the length of the bottom interface edge crack. However, G_{void} is very small for small impurity size even as the bottom crack length increases.

The success of lamination of layered solar cells can also be predicted using the differential of the interfacial energy release rates at the tips of the top and bottom interfaces. Fig. 16(a)-(b) present the prediction of successful lamination active P3HT:PCBM and MEH:PPV materials on PEDOT:PSS-glass substrate. The energy release rates are presented as a function of the normalized bottom crack length. The differential energy release rate decreases with increasing normalized bottom crack length. For a critical measured value of the interfacial energy difference, we can predict the success of the lamination such that $G_t/G_b > G_t^c/G_b^c$ for any successful lamination process and $G_t/G_b < G_t^c/G_b^c$, for unsuccessful lamination.

Author's personal copy

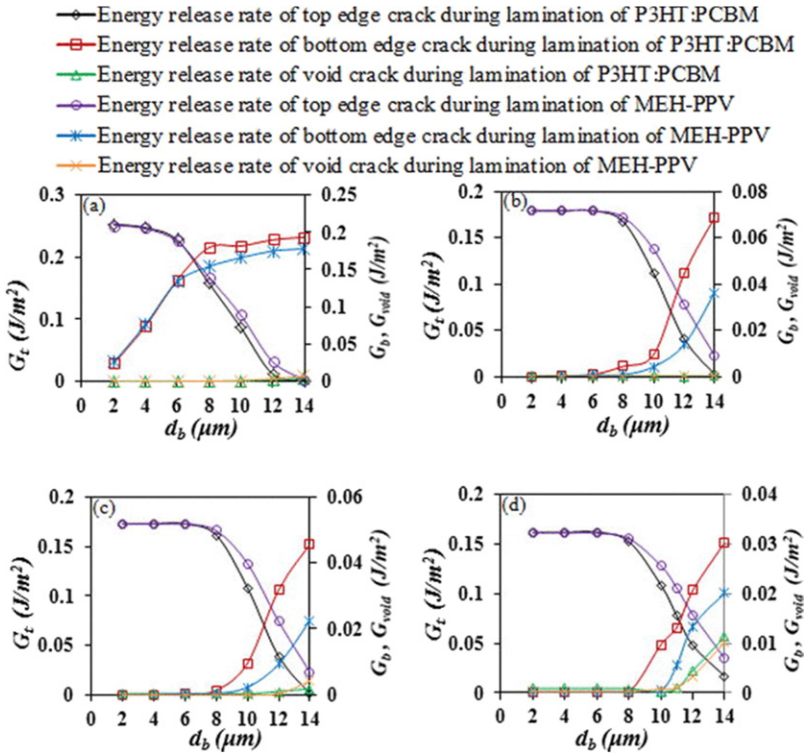

Fig. 15 Interfacial fracture during lift-up of stamp from laminated P3HT:axPCBM and MEH:PPV on PEDOT:PSS-coated substrates for different particle diameters. (a) 2 μm, (b) 6 μm, (c) 9 μ, and (d) 12 μm1. The concomitant energy release rates of the tips of the edge cracks at the top and bottom interfaces as functions of bottom crack length. Here, the length of the top edge crack is 6 μm, while the thickness of the active layers is maintained at 200 nm. Reproduced from Oyewole, O.K., Yu, D., Du, J., *et al.*, 2015. Lamination of organic solar cells and organic light emitting devices: Models and experiments. Journal of Applied Physics 118 (7). With permission from AIP Publishing.

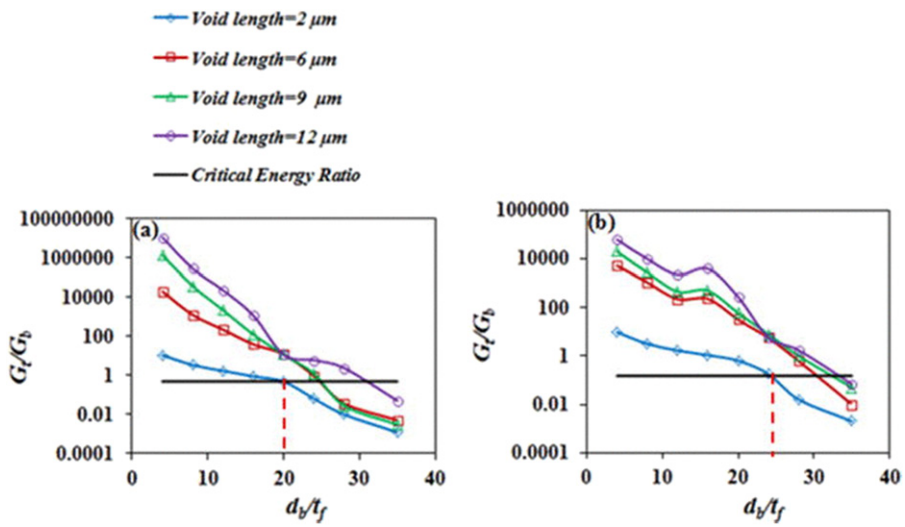

Fig. 16 Ratio of the interfacial energy release rates *Gt*/*Gb* as a function of the normalized bottom crack length (*db*/*tf*), showing the influence of the particle size for (a) lamination of P3HT:PCBM, (b) lamination of MEH-PPV. Here, the thickness of the active layer is 200 nm. Reproduced from Oyewole, O.K., Yu, D., Du, J., *et al.*, 2015. Lamination of organic solar cells and organic light emitting devices: Models and experiments. Journal of Applied Physics 118 (7). With permission from AIP Publishing.

Author's personal copy

Summary and Concluding Remarks

In this article, mechanical properties of solar cell structures have been presented. The mechanical properties of structures of conventional solar cells, organic and hybrid organic-inorganic solar cells are related to performance reliability. These properties are dependent on materials processing which greatly affects crystallinity and grain size. The mechanical strengths of silicon structures are higher for twin boundary type of crystallinity compared to processed silicon with many grains. In the case of organic and perovskite solar cells, the processing of the active materials dictates the robustness and the intermolecular interaction at the interfaces of layered structures.

The article then explored the various techniques for measuring the mechanical properties in a way that help characterization of mechanical properties of conventional and emerging solar cell structures. The mechanical properties of silicon and emerging organic and hybrid organic-inorganic solar cells structures are presented using nanoindentation technique. In the case of flexible and stretchable solar cell structure, the mechanical properties are measured under bending or stretching deformations.

The mechanical robustness of interfacial strength in emerging solar cell structures are then elucidated. Double cantilever beam, Brazil disc and peel off techniques are discussed for used in measuring interfacial fracture toughness and strengths in layered solar cell structures. These are used in reliability studies to determine weak interfaces in layered solar cell structures. The understanding of interfacial fracture toughness is then used to provide insights into the lamination of solar cells.

References

Ahn, S.-M., Jung, E.D., Kim, S.-H., *et al.*, 2019. Nanomechanical approach for flexibility of organic–inorganic hybrid perovskite solar cells. Nano Letters 19 (6), 3707–3715.

Akogwu, O., Akande, W., Tong, T., Soboyejo, W., 2011. Dendrite growth in annealed polymer blends for use in bulk heterojunction solar cells. Journal of Applied Physics 110 (10).

An, Q., Wang, J., Gao, W., *et al.*, 2020. Alloy-like ternary polymer solar cells with over 17.2% efficiency. Science Bulletin 65 (7), 538–545.

Asare, J., Agyei-Tuffour, B., Oyewole, O.K., Zebaze-Kana, G.M., Soboyejo, W.O., 2015. Deformation and failure of bendable organic solar cells. Advanced Materials Research 1132, 116–124.

Asare, J., Agyei-Tuffour, B., Amonoo, E.A., *et al.*, 2020. Effects of substrates on the performance of optoelectronic devices: A review. Cogent Engineering 7 (1).

Asif, S.A., Pethica, J.B., 2006. Nanoindentation creep of single-crystal tungsten and gallium arsenide. Philosophical Magazine A 76.

Awartani, O., Lemanski, B.I., Ro, H.W., *et al.*, 2013. Correlating stiffness, ductility, and morphology of polymer:Fullerene films for solar cell applications. Advanced Energy Materials 3 (3), 399–406.

Aziz, F., Ismail, A.F., 2015. Spray coating methods for polymer solar cells fabrication: A review. Materials Science in Semiconductor Processing 39, 416–425.

Bi, D., Li, X., Milić, J.V., *et al.*, 2018. Multifunctional molecular modulators for perovskite solar cells with over 20% efficiency and high operational stability. Nature Communications 9 (1), 4482.

Brand, V., Bruner, C., Dauskardt, R.H., 2012. Cohesion and device reliability in organic bulk heterojunction photovoltaic cells. Solar Energy Materials and Solar Cells 99, 182–189.

Bruner, C., Dauskardt, R., 2014. Role of molecular weight on the mechanical device properties of organic polymer solar cells. Macromolecules 47 (3), 1117–1121.

Cao, Y., Kim, C., Forrest, S.R., Soboyejo, W., 2005. Effects of dust particles and layer properties on organic electronic devices fabricated by stamping. Journal of Applied Physics 98 (3), 1–6.

Cheacharoen, R., Rolston, N., Harwood, D., *et al.*, 2018. Design and understanding of encapsulated perovskite solar cells to withstand temperature cycling. Energy & Environmental Science 11 (1), 144–150.

Chen, L., Xie, X., Liu, Z., Lee, E.-C., 2017. A transparent poly(3,4-Ethylenedioxylenethiophene):Poly(Styrene Sulfonate) cathode for low temperature processed, metal-oxide free perovskite solar cells. Journal of Materials Chemistry A 5 (15), 6974–6980.

Dai, Z., Yadavalli, S.K., Hu, M., *et al.*, 2020. Effect of Gworkingrain Size on the Fracture Behavior of Organic-Inorganic Halide Perovskite Thin Films for Solar Cells. Scripta Materialia 185, 47–50.

Dai, Z., Yadavalli, S.K., Chen, M., *et al.*, 2021. Interfacial Toughening with Self-Assembled Monolayers Enhances Perovskite Solar Cell Reliability. Science 372 (6542), 618–622.

Dennler, G., Forberich, K., Scharber, M.C., *et al.*, 2007. Angle dependence of external and internal quantum efficiencies in bulk-heterojunction organic solar cells. Journal of Applied Physics 102 (5), 054516.

Dianetti, M., Di Giacomo, F., Polino, G., *et al.*, 2015. TCO-free flexible organo metal trihalide perovskite planar-heterojunction solar cells. Solar Energy Materials and Solar Cells 140.

Dimesso, L., Dimamay, M., Hamburger, M., Jaegermann, W., 2014. Properties of CH3NH3PbX3 (X = I, Br, Cl) powders as precursors for organic/inorganic solar cells. Chemistry of Materials 26 (23), 6762–6770.

Docampo, P., Ball, J.M., Darwich, M., Eperon, G.E., Snaith, H.J., 2013. Efficient organometal trihalide perovskite planar-heterojunction solar cells on flexible polymer substrates. Nature Communications 4 (1), 1–6.

Dong, Q., Zhu, C., Chen, M., *et al.*, 2021a. Interpenetrating interfaces for efficient perovskite solar cells with high operational stability and mechanical robustness. Nature Communications 12 (1), 1–9.

Dong, Q., Zhu, C., Chen, M., *et al.*, 2021b. Interpenetrating interfaces for efficient perovskite solar cells with high operational stability and mechanical robustness. Nature Communications 12 (1), 973.

Dou, L., Jingbi You, Z.H., Zheng Xu, G.L., Robert, A.S., Yang, Y., 2013. 25th anniversary article: A decade of organic/polymeric photovoltaic research. Advanced Materials 25 (46), 6642–6671.

Dragišić, V.T., 2015. Silicon solar wafers: Quality control and improving the mechanical properties. Procedia Engineering 117 (1), 459–464.

Dualeh, A., Tétreault, N., Moehl, T., *et al.*, 2014. Effect of annealing temperature on film morphology of organic-inorganic hybrid pervoskite solid-state solar cells. Advanced Functional Materials 24 (21), 3250–3258.

Dupont, S.R., Oliver, M., Krebs, F.C., *et al.*, 2012. Interlayer adhesion in roll-to-roll processed flexible inverted polymer solar cells. Solar Energy Materials and Solar Cells 97.

Espinosa, N., Hösel, M., Angmo, D., Krebs, F.C., 2012. Solar cells with one-day energy payback for the factories of the future. Energy & Environmental Science 5 (1), 5117–5132.

Facchetti, A., 2013. Polymer donor-polymer acceptor (All-Polymer) solar cells. Materials Today 16 (4), 123–132.

Fan, X., Wanyi, N., Hsinhan, T., *et al.*, 2019. PEDOT:PSS for flexible and stretchable electronics: modifications, strategies, and applications. Advanced Science 6.

Feng, J., 2014a. Mechanical properties of hybrid organic-inorganic CH3NH3BX3 (B = Sn, Pb; X = Br, I) perovskites for solar cell absorbers. APL Materials 2.

Francis, L.F., Mccormick, A.V., Vaessen, D.M., *et al.*, 2002. Development and measurement of stress in polymer coatings. Journal of Materials Science 37, 4707–4731.

Galagan, Y., Rubingh, J.E.Jm, Andriessen, R., *et al.*, 2011. ITO-free flexible organic solar cells with printed current collecting grids. Solar Energy Materials and Solar Cells 95.

Gao, H., Wei, W., Li, L., Tan, Y., Tang, Y., 2020. Mechanical properties of a 2D lead-halide perovskite, (C6H5CH2NH3)2PbCl4, by nanoindentation and first-principles calculations. The Journal of Physical Chemistry C 124 (35), 19204–19211.

Author's personal copy

Gao, L., Chen, L., Huang, S., Chen, N., Yang, G., 2019. Flexible and highly durable perovskite solar cells with a sandwiched device structure. ACS Applied Materials and Interfaces 11 (19), 17475–17481.

Gerthoffer, A., Poulain, C., Roux, F., *et al.*, 2017. CIGS solar cells on ultra-thin glass substrates: Determination of mechanical properties by nanoindentation and application to bending-induced strain calculation. Solar Energy Materials and Solar Cells 166, 254–261. (November 2016).

Gouttebroze, S., Hans Ivar Lange, X.M., Ronny Gløckner, B.E., Martin Syvertsen, M.V., Ulyashin, A., 2013. Comparative analysis of mechanical properties of Si substrates processed by different routes. Physica Status Solidi ((A)) Applications and Materials Science 210 (4), 777–784.

Guo, T.-F., Pyo, S., Chang, S.-C., Yang, Y., 2001. High performance polymer light-emitting diodes fabricated by a low temperature lamination process. Advanced Functional Materials 11.

Gutwald, M., Rolston, N., Printz, A.D., *et al.*, 2020. Perspectives on intrinsic toughening strategies and passivation of perovskite films with organic additives. Solar Energy Materials and Solar Cells 209. 110433.

Hoppe, H., Sariciftci, N.S., 2004. Organic solar cells: An overview. Journal of Materials Research.

Hu, L., Wu, H., Mantia, F.L., Yang, Y., Cui, Y., 2010. Thin, flexible secondary li-ion paper batteries. ACS Nano 4 (10), 5843–5848.

Hu, Y., Niu, T., Liu, Y., *et al.*, 2021. Flexible perovskite solar cells with high power-per-weight: Progress, application, and perspectives. ACS Energy Letters. 2917–2943.

Huang, J., Li, G., Wu, E., Xu, Q., Yang, Y., 2006. Achieving high-efficiency polymer white-light-emitting devices. Advanced Materials 18 (1), 114–117.

Huseynova, G., Kim, Y.H., Lee, J.H., *et al.*, 2019. Rising advancements in the application of PEDOT:PSS as a prosperous transparent and flexible electrode material for solution-processed organic electronics. Journal of Information Display 21.

Jae, K.L., Wan, L.M., Brabec, C.J., *et al.*, 2008. Processing additives for improved efficiency from bulk heterojunction solar cells. Journal of the American Chemical Society 130.

Jian, S.R., Tseng, Y.C., Teng, I.J., Juang, J.Y., 2013. Dislocation energetics and pop-ins in AlN thin films by berkovich nanoindentation. Materials 6 (9), 4259–4267.

Jung, H.S., Han, G.S., Park, N.G., Ko, M.J., 2019. Flexible perovskite solar cells. Joule 3 (8), 1850–1880.

JY, C., AJ, N., CM, S., 2011. Surface wrinkling: A versatile platform for measuring thin-film properties. Advanced Materials 23 (3), 349–368.

Kaltenbrunner, M., White, M.S., Głowacki, E.D., *et al.*, 2012. Ultrathin and lightweight organic solar cells with high flexibility. Nature Communications 3.

Kaltenbrunner, M., Adam, G., Głowacki, E.D., *et al.*, 2015. Flexible high power-per-weight perovskite solar cells with chromium oxide–metal contacts for improved stability in air. Nature Materials 14 (10), 1032–1039.

Karagiannidis, P.G., Kassavetis, S., Pitsalidis, C., Logothetidis, S., 2011. Thermal annealing effect on the nanomechanical properties and structure of P3HT : PCBM thin films. Thin Solid Films 519 (12), 4105–4109.

Kaule, F., Wang, W., Schoenfelder, S., 2014. Modeling and testing the mechanical strength of solar cells. Solar Energy Materials and Solar Cells 120 (PART A), 441–447.

Kim, B.J., Kim, D.H., Lee, Y.Y., *et al.*, 2015a. Highly efficient and bending durable perovskite solar cells: Toward a wearable power source. Energy and Environmental Science 8.

Kim, J., Kim, K., Ko, S.H., Kim, W., 2011. Optimum design of ordered bulk heterojunction organic photovoltaics. Solar Energy Materials and Solar Cells 95 (11), 3021–3024.

Kim, T., Kim, J.H., Kang, T.E., *et al.*, 2015c. Flexible, highly efficient all-polymer solar cells. Nature Communications 6.

Kim, T., Kim, J.H., Kang, T.E., *et al.*, 2015b. Flexible, highly efficient all-polymer solar cells. Nature Communications 6, 1–7. (May).

Kim, W., Choi, J., Kim, J.-H., *et al.*, 2018. Comparative study of the mechanical properties of all-polymer and fullerene–polymer solar cells: The importance of polymer acceptors for high fracture resistance. Chemistry of Materials 30 (6), 2102–2111.

Koidis, C., Logothetidis, S., Kassavetis, S., *et al.*, 2013a. Effect of process parameters on the morphology and nanostructure of roll-to-roll printed P3HT:PCBM thin films for organic photovoltaics. Solar Energy Materials and Solar Cells Complete. 36–46. (112).

Koidis, C., Logothetidis, S., Kassavetis, S., *et al.*, 2013b. Solar energy materials & solar cells effect of process parameters on the morphology and nanostructure of roll-to-roll printed P3HT : PCBM thin films for organic photovoltaics. Solar Energy Materials and Solar Cells 112, 36–46.

Krebs, F.C., 2009. Fabrication and processing of polymer solar cells: A review of printing and coating techniques. Solar Energy Materials and Solar Cells 93.

Krebs, F.C., Nielsen, T.D., Fyenbo, J., Wadstrøm, M., Pedersen, M.S., 2010. Manufacture, integration and demonstration of polymer solar cells in a lamp for the 'Lighting Africa' initiative. Energy & Environmental Science 3 (5), 512–525.

Krebs, F.C., Jørgensen, M., Norrman, K., *et al.*, 2009. A complete process for production of flexible large area polymer solar cells entirely using screen printing-first public demonstration. Solar Energy Materials and Solar Cells 93 (4), 422–441.

Lee, I., Yun, J.H., Son, H.J., Kim, T.-S., 2017. Accelerated degradation due to weakened adhesion from Li-TFSI additives in perovskite solar cells. ACS Applied Materials & Interfaces 9 (8), 7029–7035.

Lee, J.H., Jeong, Y.R., Lee, G., *et al.*, 2018. Highly conductive, stretchable, and transparent PEDOT:PSS electrodes fabricated with triblock copolymer additives and acid treatment. ACS Applied Materials & Interfaces 10 (33), 28027–28035.

Lee, J.-Y., Connor, S.T., Cui, Y., Peumans, P., 2010. Semitransparent organic photovoltaic cells with laminated top electrode. Nano Letters 10 (4), 1276–1279.

Li, G., Zhu, R., Yang, Y., 2012. Polymer solar cells. Nature Photonics 6 (3), 153–161.

Li, H.-C., Rao, K.K., Jeng, J.Y., *et al.*, 2011. Solar energy materials & solar cells nano-scale mechanical properties of polymer/fullerene bulk hetero-junction films and their influence on photovoltaic cells. Solar Energy Materials and Solar Cells 95 (11), 2976–2980.

Li, W., Dong, H., Wang, L., *et al.*, 2014. Montmorillonite as bifunctional buffer layer material for hybrid perovskite solar cells with protection from corrosion and retarding recombination. Journal of Materials Chemistry A 2 (33), 13587–13592.

Li, Y., Meng, L., Yang, Y., *et al.*, 2016. High-efficiency robust perovskite solar cells on ultrathin flexible substrates. Nature Communications 7.

Liang, X., Ge, C., Fang, Q., *et al.*, 2021. Flexible perovskite solar cells: Progress and prospects. Frontiers in Materials 0, 17.

Lim, K.-G., Han, T.-H., Lee, T.-W., 2021. "Engineering electrodes and metal halide perovskite materials for flexible/stretchable perovskite solar cells and light-emitting diodes. Energy & Environmental Science 14 (4), 2009–2035.

Lin, Y., Firdaus, Y., Nugraha, M.I., *et al.*, 2020. 17.1% efficient single-junction organic solar cells enabled by n-type doping of the bulk-heterojunction. Advanced Science 7 (7), 1–9.

Lipomi, D.J., 2016. Stretchable figures of merit in deformable electronics. Advanced Materials 28 (22), 4180–4183.

Lipomi, D.J., Bao, Z., 2011. Stretchable, elastic materials and devices for solar energy conversion. Energy & Environmental Science 4 (9), 3314–3328.

Lipomi, D.J., Tee, B.C.K., Vosgueritchian, M., Bao, Z., 2011. Stretchable organic solar cells. Advanced Materials 23 (15), 1771–1775.

Liu, M., Johnston, M.B., Snaith, H.J., 2013. Efficient planar heterojunction perovskite solar cells by vapour deposition. Nature 501 (7467), 395–398.

Liu, Y., Qi, N., Song, T., *et al.*, 2014. Highly flexible and lightweight organic solar cells on biocompatible silk fibroin. ACS Applied Materials and Interfaces 6 (23), 20670–20675.

Ma, L., Li, W., Yang, K., *et al.*, 2021. A- or X-site mixture on mechanical properties of APbX3 perovskite single crystals. APL Materials 9 (4), 041112.

Malliaras, G., Friend, R., 2005. An organic electronics primer. Physics Today 58 (5), 53–58.

Mamun, A.A., Mohammed, Y., Ava, T.T., Namkoong, G., Elmustafa, A.A., 2018. Influence of air degradation on morphology, crystal size and mechanical hardness of perovskite film. Materials Letters 229, 167–170.

Manser, J.S., Christians, J.A., Kamat, P.V., 2016. Intriguing optoelectronic properties of metal halide perovskites. Chemical Reviews 116 (21), 12956–12958.

Meng, L., Zhang, Y., Wan, X., *et al.*, 2018. Organic and solution-processed tandem solar cells with 17.3% efficiency. Science 361 (6407), 1094–1098.

Merritt, V.Y., Hovel, H.J., 1976. Organic solar cells of hydroxy squarylium. Applied Physics Letters 29 (7), 414–415.

Modi, M.B., Sitaraman, S.K., 2004. Interfacial fracture toughness measurement for thin film interfaces. Engineering Fracture Mechanics 71 (9–10), 1219–1234.

Müller, C., Goffri, S., Breiby, D.W., *et al.*, 2007. Tough, semiconducting polyethylene-poly(3-Hexylthiophene) diblock copolymers. Advanced Functional Materials 17 (15), 2674–2679.

Murali, B., Saidaminov, M.I., Abdelhady, A.L., *et al.*, 2016. Robust and air-stable sandwiched organo-lead halide perovskites for photodetector applications. Journal of Materials Chemistry C 4 (13), 2545–2552.

Nehm, F., Pfeiffelmann, T., Dollinger, F., Müller-Meskamp, L., Leo, K., 2017. Influence of aging climate and cathode adhesion on organic solar cell stability. Solar Energy Materials and Solar Cells 168, 1–7.

Author's personal copy

NREL. 2020. "National Renewable Energy Laboratory Photovoltaic Research: Best Research-Cell Efficiency Chart." Best Research-Cell Efficiency Chart | Photovoltaic Research | NREL.
O'Connor, B., Chan, E.P., Chan, C., *et al*., 2010. Correlations between mechanical and electrical properties of polythiophenes. ACS Nano 4 (12), 7538–7544.
Oh, J.Y., Jang, W.S., Lee, T.Il, Myoung, J.-M., Baik, H.K., 2011. Driving vertical phase separation in a bulk-heterojunction by inserting a poly(3-Hexylthiophene) layer for highly efficient organic solar cells. Applied Physics Letters 98 (2), 023303.
Oyelade, O.V., Oyewole, O.K., Oyewole, D.O., *et al*., 2020. Pressure-assisted fabrication of perovskite solar cells. Scientific Reports 10 (1), 1–11.
Oyewole, O.K., Yu, D., Du, J., *et al*., 2015. Lamination of organic solar cells and organic light emitting devices: Models and experiments. Journal of Applied Physics 118 (7).
Oyewole, O., Oyewole, D., Oyelade, O., *et al*., 2020. Failure of stretchable organic solar cells under monotonic and cyclic loading. Macromolecular Materials and Engineering 305 (11), 2000369.
Pascoe, A.R., Yang, M., Kopidakis, N., *et al*., 2016. Planar versus mesoscopic perovskite microstructures: The influence of CH3NH3PbI3 morphology on charge transport and recombination dynamics. Nano Energy 22.
Philip, J., Hariskos, D., Lotter, E., *et al*., 2010. "New world record efficiency for Cu(In,Ga)Se2 thin-film solar cells beyond 20%. Progress in Photovoltaics 19 (6), 894–897.
Popoola, I.K., Gondal, M.A., Qahtan, T.F., 2018. Recent progress in flexible perovskite solar cells: Materials, mechanical tolerance and stability. Renewable and Sustainable Energy Reviews 82.
Popovic, Z.D., Loutfy, R.O., 1981. Transient photoresponse measurements in X-phase of metal-free phthalocyanine photovoltaic cells. Journal of Applied Physics 52 (10), 6190–6196.
Popovich, V.A., Yunus, A., Janssen, M., Richardson, I.M., Bennett, I.J., 2011. Effect of silicon solar cell processing parameters and crystallinity on mechanical strength. Solar Energy Materials and Solar Cells 95 (1), 97–100.
Popovich, V.A., Riemslag, A.C., Janssen, M., Bennett, I.J., Richardson, I.M., 2013. Characterization of multicrystalline silicon solar wafers fracture strength and influencing factors. International Journal of Material Science 3 (1), 9–17.
Printz, A.D., Zaretski, A.V., Savagatrup, S., *et al*., 2015. Yield point of semiconducting polymer films on stretchable substrates determined by onset of buckling. ACS Applied Materials & Interfaces 7.
Rakita, Y., Cohen, S.R., Kedem, N.K., Hodes, G., Cahen, D., 2015. Mechanical properties of APbX 3 (A = Cs or CH 3 NH 3 ; X = I or Br) perovskite single crystals. MRS Communications 5, 623–629.
Ramirez, C., Yadavalli, S.K., Garces, H.F., Zhou, Y., Padture, N.P., 2018. Thermo-mechanical behavior of organic-inorganic halide perovskites for solar cells. Scripta Materialia 150, 36–41.
Rathore, S., Han, G., Kumar, A., Leong, W.L., Singh, A., 2021. Elastic modulus tailoring in CH3NH3PbI3 perovskite system by the introduction of two dimensionality using (5-AVA)2PbI4. Solar Energy 224, 27–34.
Reyes-Martinez, M.A., Abdelhady, A.L., Saidaminov, M.I., *et al*., 2017a. Time-dependent mechanical response of APbX3 (A = Cs, CH3NH3; X = I, Br) single crystals. Advanced Materials 29.
Rodriquez, D., Kim, J.-H., Root, S.E., *et al*., 2017. Comparison of methods for determining the mechanical properties of semiconducting polymer films for stretchable electronics. ACS Applied Materials and Interfaces 9 (10), 8855–8862.
Roldán-Carmona, C., Malinkiewicz, O., Soriano, A., *et al*., 2014. Flexible high efficiency perovskite solar cells. Energy and Environmental Science 7 (3), 994–997.
Rolston, N., Watson, B.L., Bailie, C.D., *et al*., 2016a. Mechanical integrity of solution-processed perovskite solar cells. Extreme Mechanics Letters 9, 353–358.
Rolston, N., Printz, A.D., Tracy, J.M., *et al*., 2018. Effect of cation composition on the mechanical stability of perovskite solar cells. Advanced Energy Materials 8 (9), 1702116.
Root, S.E., Savagatrup, S., Printz, A.D., Rodriquez, D., Lipomi, D.J., 2017. Mechanical properties of organic semiconductors for stretchable, highly flexible, and mechanically robust electronics. Chemical Reviews 117 (9), 6467–6499.
Soufiani, A.M., Hameiri, Z., Meyer, S., *et al*., 2017. Lessons learnt from spatially resolved electro- and photoluminescence imaging: Interfacial delamination in CH 3 NH 3 PbI 3 planar perovskite solar cells upon illumination. Advanced Energy Materials 7 (9), 1602111.
Stafford, C.M., Harrison, C., Beers, K.L., *et al*., 2004. A buckling-based metrology for measuring the elastic moduli of polymeric thin films. Nature Materials 3.
Suchol Savagatrup, A.D.P., O'Connor, T.F., Zaretski, A.V., *et al*., 2014. Mechanical degradation and stability of organic solar cells: Molecular and microstructural determinants. Energy & Environmental Science 8 (1), 55–80.
Sum, T.C., Mathews, N., 2014. Advancements in perovskite solar cells: Photophysics behind the photovoltaics. Energy & Environmental Science 7 (8), 2518–2534.
Sun, C., Pan, F., Bin, H., *et al*., 2018. A low cost and high performance polymer donor material for polymer solar cells. Nature Communications 9 (1), 1–10.
Sun, S., Fang, Y., Kieslich, G., White, T.J., Cheetham, A.K., 2015a. Mechanical properties of organic-inorganic halide perovskites, CH3NH3PbX3 (X = I, Br and Cl), by nanoindentation. Journal of Materials Chemistry A 3 (36), 18450–18455.
Sun, S., Isikgor, F.H., Deng, Z., *et al*., 2017. Factors influencing the mechanical properties of formamidinium lead halides and related hybrid perovskites. ChemSusChem 10 (19), 3740–3745.
Sun, S., Salim, T., Mathews, N., *et al*., 2013. The origin of high efficiency in low-temperature solution-processable bilayer organometal halide hybrid solar cells. Energy & Environmental Science 7 (1), 399–407.
Tan, J.C., Cheetham, A.K., 2011. Mechanical properties of hybrid inorganic–organic framework materials: Establishing fundamental structure–property relationships. Chemical Society Reviews 40 (2), 1059–1080.
Tang, C.W., 1986. Two-layer organic photovoltaic cell. Applied Physics Letters 48 (2), 183–185.
Tang, C.W., AlBrecht, A.C., 2008. Photovoltaic effects of metal – Chlorophyll-a – Metal sandwich cells. The Journal of Chemical Physics 62. 2139. (September).
Tang, H., Feng, H., Wang, H., *et al*., 2019. Highly conducting MXene–silver nanowire transparent electrodes for flexible organic solar cells. ACS Applied Materials & Interfaces 11 (28), 25330–25337.
Tank, D., Lee, H.H., Khang, D.Y., 2009. Elastic moduli of organic electronic materials by the buckling method. Macromolecules 42 (18), 7079–7083.
Thote, A., Jeon, Il, Lee, J.W., *et al*., 2019. Stable and reproducible 2D/3D formamidinium-lead-iodide perovskite solar cells. ACS Applied Energy Materials 2 (4), 2486–2493.
Tong, T., Babatope, B., Admassie, S., *et al*., 2009. Adhesion in organic electronic structures. Journal of Applied Physics 106 (8).
Tong, T.M., Tan, T., Rahbar, N., Soboyejo, W.O., 2014. Mode mixity dependence of interfacial fracture toughness in organic electronic structures. IEEE Transactions on Device and Materials Reliability 14 (1), 291–299.
Tu, Q., Spanopoulos, I., Hao, S., *et al*., 2018a. Out-of-plane mechanical properties of 2D hybrid organic-inorganic perovskites by nanoindentation. ACS Applied Materials and Interfaces 10 (26), 22167–22173.
Tucker, M.B., Hines, D.R., Teng, Li, 2009. A quality map of transfer printing. Journal of Applied Physics 106 (10), 103504.
Venkateswararao, A., Liu, S.W., Wong, K.T., 2018. Organic polymeric and small molecular electron acceptors for organic solar cells. Materials Science and Engineering R: Reports 124, 1–57.
Wang, H., Zhu, C., Liu, L., *et al*., 2019a. Interfacial residual stress relaxation in perovskite solar cells with improved stability. Advanced Materials 31 (48), 1904408.
Wang, M., Xie, F., Du, J., *et al*., 2011. Degradation mechanism of organic solar cells with aluminum cathode. Solar Energy Materials and Solar Cells 95 (12), 3303–3310.
Wang, P., Wu, Y., Cai, B., *et al*., 2019b. Solution-processable perovskite solar cells toward commercialization: Progress and challenges. Advanced Functional Materials 29 (47), 1807661.
Wang, S.-H., Hsiao, Y.-J, Wang, S.-H., *et al*., 2013. Enhancing performance and nanomechanical properties of carbon nanotube doped P3HT:PCBM solar cells. ECS Journal of Solid State Science and Technology 2.
Weinberger, B.R., Akhtar, M., Gau, S.C., 1982. Polyacetylene photovoltaic devices. Synthetic Metals 4 (3), 187–197.
White, M.S., Kaltenbrunner, M., Głowacki, E.D., *et al*., 2013. Ultrathin, highly flexible and stretchable PLEDs. Nature Photonics 7 (10), 811–816.
Wu, H., Melkote, S.N., 2013. Effect of crystal defects on mechanical properties relevant to cutting of multicrystalline solar silicon. Materials Science in Semiconductor Processing 16 (6), 1416–1421.
Wu, X., 2004. High-efficiency polycrystalline CdTe thin-film solar cells. Solar Energy 77 (6), 803–814.

Author's personal copy

Wu, Z., Li, P., Zhang, Y., Zheng, Z., 2018. Flexible and stretchable perovskite solar cells: Device design and development methods. Small Methods 2 (7), 1800031.
Xiong, H., DeLuca, G., Rui, Y., *et al*., 2018. Modifying perovskite films with polyvinylpyrrolidone for ambient-air-stable highly bendable solar cells. ACS Applied Materials & Interfaces 10 (41), 35385–35394.
Yambem, S.D., Liao, K.S., Curran, S.A., 2012. Enhancing current density using vertically oriented organic photovoltaics. Solar Energy Materials and Solar Cells 101, 227–231.
Yang, D., Yang, R., Priya, S., *et al*., 2019. Recent advances in flexible perovskite solar cells: Fabrication and applications. Angewandte Chemie - International Edition 58.
Ye, L., Xiong, Y., Zhang, Q., *et al*., 2018. Surpassing 10% efficiency benchmark for nonfullerene organic solar cells by scalable coating in air from single nonhalogenated solvent. Advanced Materials 30 (8), 1–9.
Yongjin, K., 2013. Experiental Investigation of the Interfacial Fracture Toughness in Organic Photovoltaics. Georgia institute if technology.
Yu, D., Oyewole, O.K., Kwabi, D., *et al*., 2014. Adhesion in flexible organic and hybrid organic/inorganic light emitting device and solar cells. Journal of Applied Physics 116 (7).
Yu, J., Wang, M., Lin, S., 2016a. Probing the soft and nanoductile mechanical nature of single and polycrystalline organic–inorganic hybrid perovskites for flexible functional devices. ACS Nano 10 (12), 11044–11057.
Yun, J.H., Lee, I., Kim, T.-S., *et al*., 2015. Synergistic enhancement and mechanism study of mechanical and moisture stability of perovskite solar cells introducing polyethylene-imine into the CH 3 NH 3 PbI 3/HTM interface. Journal of Materials Chemistry A 3 (44), 22176–22182.
Zardetto, V., Brown, T.M., Reale, A., Carlo, A.Di, 2011. Substrates for flexible electronics: A practical investigation on the electrical, film flexibility, optical, temperature, and solvent resistance properties. Journal of Polymer Science Part B: Polymer Physics 49 (9), 638–648.
Zarick, H.F., Soetan, N., Erwin, W.R., Bardhan, R., 2018. Mixed halide hybrid perovskites: A paradigm shift in photovoltaics. Journal of Materials Chemistry A 6.
Zhang, R., Moon, K.S., Lin, W., Agar, J.C., Wong, C.P., 2011. A simple, low-cost approach to prepare flexible highly conductive polymer composites by in situ reduction of silver carboxylate for flexible electronic applications. Composites Science and Technology 71 (4), 528–534.
Zhang, Y., Wu, Z., Li, P., *et al*., 2018a. Fully solution-processed TCO-free semitransparent perovskite solar cells for tandem and flexible applications. Advanced Energy Materials 8 (1), 1701569.
Zhang, Z., Lv, R., Jia, Y., *et al*., 2018b. All-carbon electrodes for flexible solar cells. Applied Sciences 8 (2).
Zhao, W., Li, S., Yao, H., *et al*., 2017. Molecular optimization enables over 13% efficiency in organic solar cells. Journal of the American Chemical Society 139 (21), 7148–7151.
Zhu, C., Meng, L., Zhang, J., *et al*., 2021. A quinoxaline-based D–A copolymer donor achieving 17.62% efficiency of organic solar cells. Advanced Materials 33 (23), 2100474.